The Big Bang Never Happened—A Reassessment of the Galactic Origin of Light Elements (GOLE) Hypothesis and its Implications

Eric J. Lerner

LPPFusion, 128 Lincoln Blvd., Middlesex, NJ, USA, 08846

Abstract: The growing list of failed predictions of the inflationary ΛCDM theory is a widely-recognized crisis in cosmology. It is therefore timely to re-examine if the Big Bang hypothesis (BBH), which underlies the dominant cosmological model, is valid. The core of that hypothesis is that the universe began with a short period of extremely high temperature and density. Such a hot, dense epoch produces light elements by fusion reactions. But the actual published predictions of the Big Bang Nucleosynthesis (BBN) theory of light element production have increasingly diverged from observations. The predictions for both lithium and helium abundance now differ by many standard deviations from observations, a situation that is worsening at an accelerating pace. Only deuterium predictions have remained in agreement with observation. In contrast, the published predictions of the alternative hypothesis, that all light elements were created by thermonuclear and cosmic ray processes in young galaxies, have been repeatedly confirmed by observations. This paper reassesses the galactic origin of light element (GOLE) hypothesis in light of new calculations and recent observations. The GOLE predictions remain in good agreement with all relevant elemental abundance data sets and are contradicted by none. As well, the expansion of space required by the BBH is directly contradicted by both data on surface brightness and supernova light curves. Nor are any of the quantitative predictions of BBH for the CMB in accord with observations, while GOLE provides an alternative explanation for the CMB that requires none of the BBH's hypothetical entities, such as dark matter or dark energy. BBH predictions are contradicted by 16 different data sets while GOLE predictions are contradicted by none. The solution to the crisis in cosmology is to abandon the Big Bang hypothesis.

Key words: Light elements; surface brightness; cosmology: theory; Big Bang

1. Introduction: Was there a hot dense Big Bang?

A key hypothesis of concordance cosmology is that the universe began with a brief epoch of extremely high temperature and density, the Big Bang. The most direct test of the validity of this theory is in comparing its predictions with the abundance of certain light elements, since if the universe went through a brief period of high density and temperature, thermonuclear reactions would inevitably produce helium, deuterium and lithium in specific amounts that depend only on the ratio of photons to baryons.

It has been repeatedly claimed by many authors that the predictions of the theory have been confirmed by observation and thus that the hypothesis is valid (for example, Mathews, Kusakabe, & Kajino 2017). But an objective assessment of the abundant literature leads to the opposite conclusion, that observations contradict the predictions and that improved observations

have increased this contradiction, invalidating the hypothesis. Since this conclusion is opposed to many published claims, this paper presents in section 2 an in-depth analysis of this divergence of predictions and observations. We then, in section 3, show that the GOLE hypothesis has correctly predicted observations and in section 4 that the agreement still exists and has improved with time.

Since the BBH is widely claimed to be indirectly supported by many other data sets, including evidence of the expansion of the universe, a full test of its validity must examine these claims, as well as testing if the GOLE hypothesis is compatible with these other data sets. The implications of the GOLE and BBH for the antimatter problem are examined in section 5; for the expansion of the universe and the surface brightness test in section 6; and for supernova light curves in section 7. The results are discussed in section 8 and conclusions arrived at in section 9.

2. Big Bang Nucleosynthesis Predictions have been refuted by Observation

Over a period of many decades, but in recent years at an accelerating pace, actual observations have consistently and severely diverged from the light elements abundance predictions derived from Big Bang Nucleosynthesis (BBN) theories. Yet, although the accord of observations with predictions should have been viewed as a critical test of the Big Bang, the increasing divergence of observation and prediction has not generally been viewed as a failure of the Big Bang, but rather as a persistently unexplained anomaly.

In testing BBN predictions against observations, it is essential to perform a chronological analysis, comparing published predictions with *subsequent* observations. It is always possible to create explanations of some sort for observations that have *already* been made—see, for example Kipling (1912). But this is not science, which requires validation by predictions made before observations.

It should be noted that the abundance of light elements was not the first data set hypothesized as evidence for the Big Bang. In the very first proposal of the Big Bang hypothesis George Lemaitre (1931) cited the observation of high-energy cosmic rays as the key observational evidence for a "primeval atom" which burst apart at energies above those that could be achieved by any process in the present-day universe. But Millikan had already demonstrated in 1928 that most cosmic rays observed on earth could be produced by nuclear reactions (Millikan and Cameron,1928). By 1939, Alfven (1939) demonstrated that magnetic fields in the galaxy would so scramble the directions of cosmic rays that they should become isotropic.

In 1946, Gamow (1946) proposed that the abundance of the elements, both heavy and light, could be predicted from a hot, dense, rapidly expanding origin of the universe, with only the density of the universe at a given time as a free variable. Once again, these predictions were almost immediately refuted. Hoyle (1946) showed that stellar evolution would lead to the production of heavier and heavier elements as the temperature in the center of a star increased. Far more detailed calculations ten years later by Burbidge, Burbidge, Fowler and Hoyle (Burbidge, et al 1957) showed that all the elements could be produced in roughly the right amounts by stars in the galaxy. As with cosmic rays, a phenomenon adduced as evidence of a

Big Bang could be predicted in far greater and more accurate detail by processes in the current universe, specifically by stellar nucleosynthesis.

The abundance of light elements was first hypothesized to be a consequence of the Big Bang in 1964 when Hoyle and Taylor (1964) published new calculations that indicated that ^{4}He,would be produced in approximately the observed amount by a Big Bang, although the predicted value was 39% by mass, which turned out to be considerably too high. Wagoner, Fowler and Hoyle (1967) showed in much greater detail that Big Bang predictions for the abundance of ^{4}He, ^{3}He, D and ^{7}Li could be obtained only dependent on the universal density of matter (Fig.1). Since the density variable was not at all easy to measure observationally with minimal accuracy, the predictions of BBN reduced to the existence of a range of density, η, that would give abundance predictions for all four isotopes that were consistent with observations.

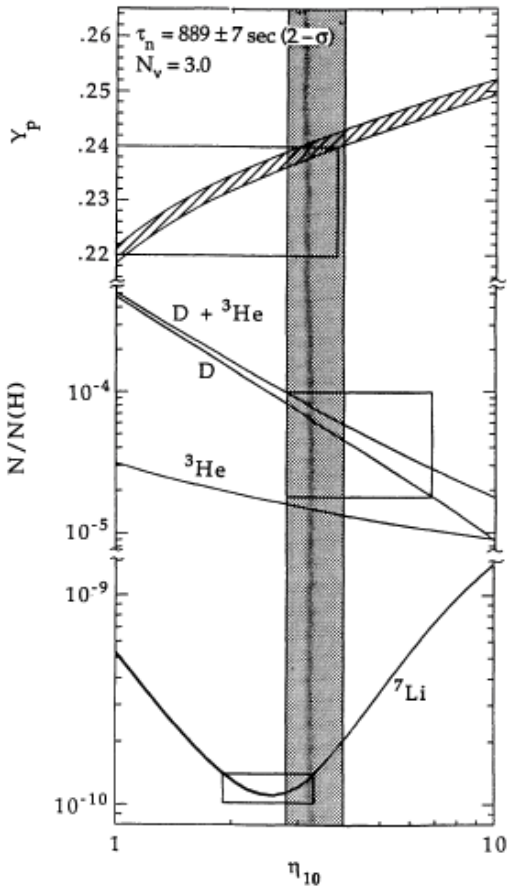

Fig. 1. BBN predictions of abundance of light elements vs nucleon to photon ratio times 10^{10}, from Walker et al (1991). The boxes showed those authors' estimates of observations and the vertical band is the range of η compatible with them. Actually, it is only the narrower range, $2.7<\eta<3.3$, to the left of the dark vertical line (in the original figure) that is compatible with all three boxes.

In the first 15 years after these predictions were made, observed data provided only relatively wide ranges to compare with predictions. As a result, during this period there was no gap between the broad predictions of BBN and the equally broad range of observed abundances.

But by the early 1980's this situation began to change, with much better data becoming available for all four isotopes. In 1982 Spite and Spite (1982) discovered a consistent Li abundance of close to 1.6 $x10^{-10}$ in Pop II dwarfs with a range of low heavy-elemental abundances. In the same period, measurements of ^{4}He abundances in H II regions started to accumulate evidence the ^{4}He abundance was no higher than 23% (Yang et al, 1984). As well, observations of D in interstellar plasma towards stars in the galaxy indicated upper limits for D around $2x10^{-5}$.

As early as 1984, Vida-Madaj and Gry (1984) concluded that the observational results "seem to fit poorly the prediction of the standard Big Bang nucleosynthesis model." They found that He observation required $0.3<\eta<3$ while observation for D require a range of $3.5<\eta<20$, with Li in between. Already the gap between the He and D observations was about 2σ.

In 1986 Ferland, (1986) calculated new collisional corrections that reduced the lowest ^{4}He values to 18.6%. Melnick et al (1992) reported an observation as low as 21.6+-0.6% in 1992 while Mathews, Boyd and Fuller (1993) extrapolated data from over 40 galaxies plotted in Y vs Z to obtain a similar value of 22.3+-0.6%. Based on this and similar observations, the present author pointed out (Lerner, 1993) that ^{4}He could be, even at a 2σ limit, no more than 23%, which by BB calculations would imply primordial D of $1.7x10^{-4}$. This would be about 8 times the level observed in the ISM, requiring massive destruction of D in stars. Multiple observations showed this could not be the case because such thorough processing would produce wide variations in D and ^{3}He, which were not observed, and would over-produce ^{4}He, C,N and O. Walker et al (1991) claimed consistency in the narrow range of $2.7<\eta<3.3$, as shown in Fig.1, but only by allowing a ^{4}He abundance of 24%.

The failure of BBN predictions was acknowledged by Steigman, (1995) who termed it an "emerging crisis" and concluded that "the standard model of BBN" conflicted with observations at a 99.7% level. However, it should be noted that the author did not see this as evidence against the validity of BBN, but merely that some unknown physics, such as a massive tau neutrino, might modify the predictions.

In 1997, Izotov et al (1997) began a series of papers that argued for a considerably higher observational value of ^{4}He, 24.3%, thus lifting η to 3.5 and relieving tension with the D and Li abundances. However, Izotov et al arrived at this higher figure mainly by either selecting out, for various reasons, or not including in the first place, all of the HII regions with the lowest ^{4}He abundances**.** This introduced a strong confirmation bias in the sample selection itself. Such selection was only deemed necessary after it was clear that lower ^{4}He abundances contradicted BBN.

Three developments in the first decade of the 21st century significantly increased the distance between BBN predictions and observations. First, calculations based on the angular power spectrum of the CMB, as measured first by BOOMERANG and later by WMAP led to a prediction of η of about 6.4. **(**Bennet et al, 2003**)** This was *nearly a factor of two higher* than the

value calculated on the basis of BBN theory and abundance measurements. If the BBN calculations were taken as a prediction of the results based on the CMB, it was a wrong prediction. On the positive side, the new value of gave BBN predictions for D abundance that were much lower than previous ones, around $2.7x10^{-5}$, and thus more in line with observations. This was the one valid prediction of the theory.

However, the discrepancy between BBN predictions and both ^{4}He and Li observations was thus increased. The predicted ^{4}He abundance rose to over 24.8% and the predicted ^{7}Li to $3.76x\ 10^{-10}$. As Cyburt, Fields and Olive (2003), among others, pointed out, the ^{4}He predictions *were now higher than any prior observational determination of abundance* and more than the values of most of the individual HII regions observed. The prediction was already 2.8 σ way from even Izotov's value, and much further from others. For ^{7}Li, the difference was over 6 σ. However, Cyburt *et al* did not consider this evidence against BBN, but rather evidence for either unknown systematic effects on the observations or "new physics".

Second, by 2007 new data sets allowed the indirect measurement of ^{4}He abundances in nearby stars (Casagrande, et al, 2007). For stars with accurate parallaxes, the absolute luminosity, spectroscopically measured metallicity, and surface temperature could be combined to give an accurate measure of ^{4}He abundance in K dwarf stars. Casagrande *et al* found that when these Y results were plotted against Z, the slope turned down sharply below Z=0.013, with the zero intercept below around 10%. Just the five stars with lowest metallicity had a mean Y of 13.6+-1.3%, more than 8 σ below the BBN predictions.

Third, at nearly the same time, observations of increasingly metal-deficient stars showed that as Fe abundance declined, so did ^{7}Li abundance, even below the Spite plateau. The discovery of HE 1327-2326, with an upper limit for A(^{7}Li) initially reported as <1.5, and subsequently lowered to <0.75, with an [Fe/H] of -5.75, opened up a yawning gap of more than a factor of 100 between BBN predictions and observations (Piau *et al,* 2006). Previous theories of Li depletion prior to the formation Spite plateau stars had, of course, predicted that the purest stars would have higher Li abundance, to accord with BBN predictions. Instead, observations showed much *lower* Li abundances.

During the past decade, the gap between observations of ^{4}He and Li abundances and BBN predictions has only grown, and at an accelerating pace as observations have improved and analysis has confirmed the implications of these observations. In 2010 Portinari, Casagrande and Flynn (2010) used homology relations to confirm the previous analysis of HR diagrams and showed that this analysis led to a dY/dZ slope of about 10 for Z<0.015 and a primordial He value of 11%. (Fig.2) The authors, again accepting BBN as indisputable, attempted various ways of explain the discrepancy, which they called the "low helium problem", in terms of possible errors in stellar theory but were unable to come up with a satisfactory fix. This situation remains unchanged at present.

Since He and age have opposing effects on a star's position in the HR diagram, stars with apparently low He can be interpreted as having higher He but also being much older, as Valcarce *et al* (2013) pointed out. However, for all stars to have He abundances>0.245, ages as old as 50 Gy must be hypothesized, which is precluded by the BBH.

In addition, more comprehensive catalogs of planetary nebulae and HII regions in the Local Group (Maciel, Costa and Cavichia 2017) show helium abundances measured *spectroscopically* extending down to 11% by mass, completely confirming the analysis from local stars. No papers in the literature provide an explanation of the more than factor of 2 gap between observations of He abundance and the lowest primordial He values predicted by the BBH.

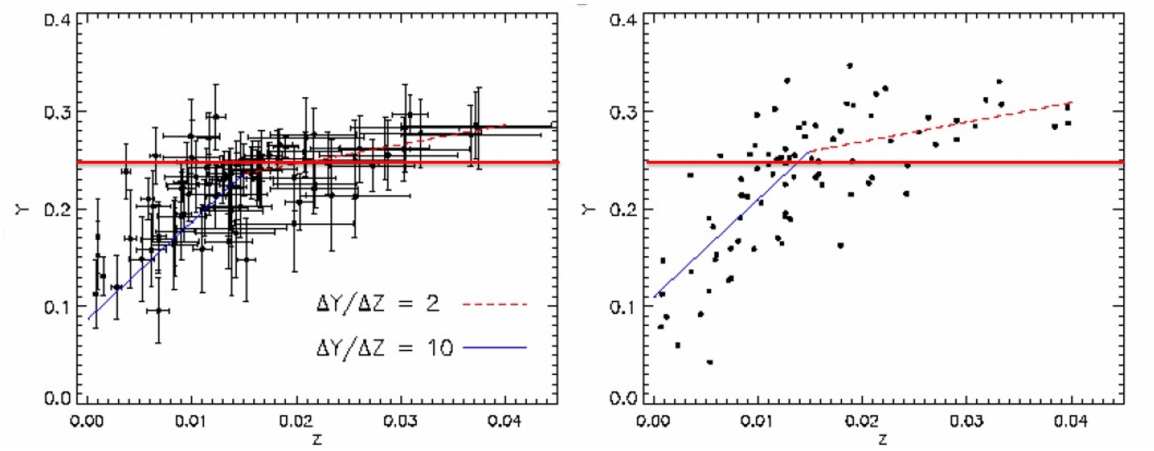

Figure 2. Observed He/H mass ratios vs metallicity ratio z for nearby field dwarfs from Portinari et al (2010) Left panel: using the isochrone fitting procedure described in Casagrande et al. (2007). Right panel: using numerical homology relations.

Even limiting the comparison to analysis of low-metallicity galaxies still leads to a contradiction with the increasing precise predictions from BBH based on CMB observations. The Planck 2018 prediction of 24.69+-0.02% He (Planck Collaboration, 2020) is 3 σ above the latest analysis of low-metallicity galaxies (Matsumoto et al, 2022) which gives 23.8+-0.3%. It should again be emphasized that this analysis is strongly biased upwards because galaxies are only included if eight He lines are measurable, which excludes those with the lowest He abundances and faintest lines and as well excludes all upper limit estimates. It also should be noted that while the Matsumoto value of He abundance I only 3.6% below the Planck prediction, the η value of baryon density compatible under BBN with the Matusumoto value is a **factor of two** below that required by the BB CMB theory.

Similarly, the even larger gap between observation and prediction continued to grow with Li. Observations in the past dozen years have filled in the gap between the Spite plateau and HE 1327-2326, showing clearly that for an [Fe/H] <-3.5 there is an steepening slope for A(Li) on[Fe/H]. As shown in Fig. 3**,** a linear plot Li vs Fe abundance in ppb of H of all 26 stars with [Fe/H] <-3.5 shows a steepening slope, best fit empirically by a power law, A(Li)= 0.34 [Fe/H]+3.16 with a high correlation coefficient r= 0.72. (Here all points with only upper limits for A(Li) are plotted as being at these upper limits). The scatter is entirely consistent with observational uncertainties.

If we take a linear fit to the 13 lowest-Fe stars with an Fe/H ratio of less than 5 ppb, the zero intercept for Li/H is 2.5+_0.9x10^{-11} which is thus 47 σ from the BBN prediction of 4.6-5.3x10^{-10}.

Even without statistical analysis, it is clear at a glance from Fig.3 that the BBN predictions are falsified by the data. The prediction is at least 20 times larger than the observation. As Fields et al (2020) concluded (final paragraph of paper), in accord with many other papers, ”There is a clear mismatch between the BBN predicted abundance and the abundance seen in metal-poor stars.”

The so-called “lithium problem” has been widely recognized in the literature (see, e.g. Mathews et al (2020) for a survey) but attempts to solve it either by ideas in nuclear physics, “new physics”—ad hoc assumptions about early cosmic evolution-- or stellar evolution have so far not succeeded. All of these efforts are aimed at somehow explaining a depletion of lithium from the BBH predicted level to the one actually observed. The key problem faced in these efforts is evident from Fig 3. There are no stars observed in the white gap between the data points and the BBH predictions. How can a process starting at the level of the red lines reduce some stellar Li abundances down 20 times without producing any stars at lesser depletions? In other words, how can a narrow observed abundance distribution with a width of at most +-0.025 ppb (at most, since it is consistent with observational uncertainty) be produced by a process that reduces abundance by a 20 times larger amount?

As Tognelli *et al* (2020) point out “all hypotheses based on stellar physics and evolution that are used to explain the cosmological Li discrepancy need to resort, to different degrees, to fine tuning and/or ad hoc assumptions.” Examples of such assumptions are non-physically-motivated turbulent layers and fine-tuned stellar accretion rates. To successfully explain the observed Li abundances, a theory would have to, at least, first account quantitatively for the observed decrease of Li with decreasing Fe; second, make other predictions that are in accord with other observations and third, make no predictions contradicted by observations. To be validated, such a theory would also have to make new predictions of some subsequent observations. But no papers have so far been able to even satisfy the first three minimum criteria. Nor have any papers in the literature used BBH, however modified with additional hypotheses, to actually *predict* the observational results that show a decline in Li abundance with declining heavy metal abundance to levels far below BBH predictions and compatible with zero initial Li. As pointed out in section 2, only predictions from hypotheses made *prior* to observations can be used to test the validity of the hypotheses. On this basis, there is a factor of 20 between Li abundance predictions and observations.

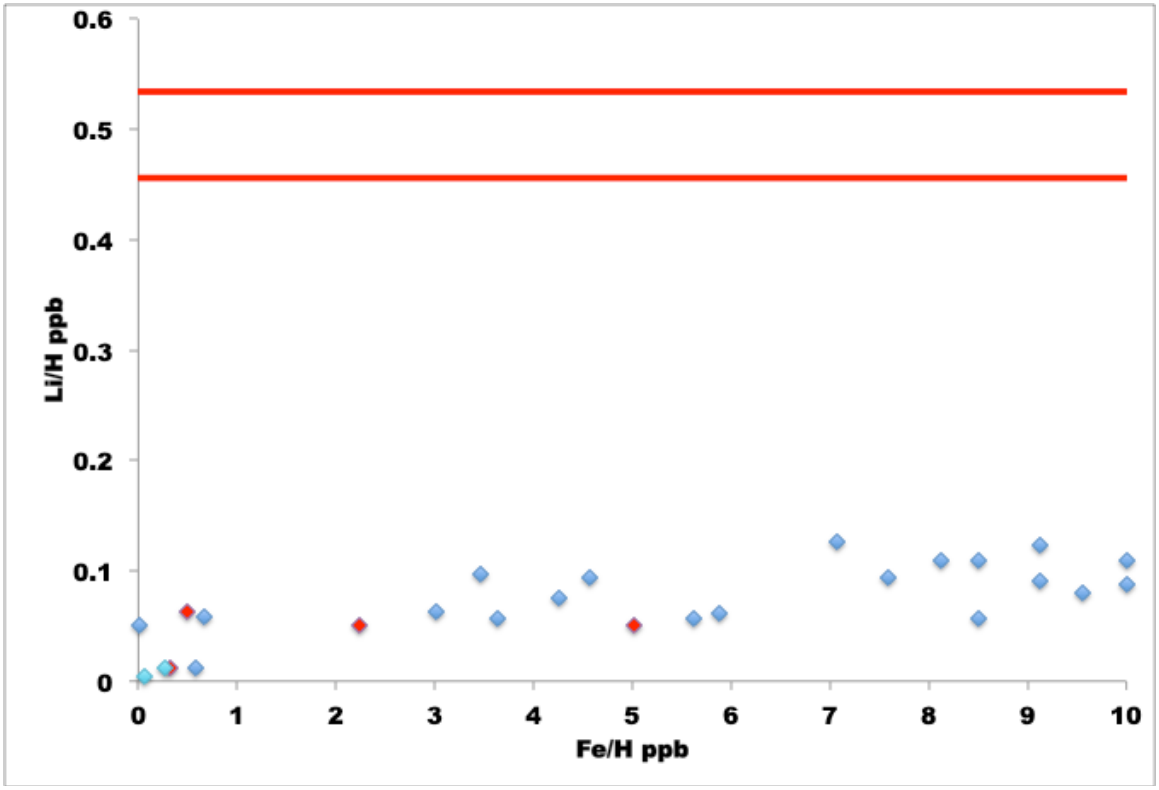

Fig. 3. Li vs Fe abundance for the 26 known dwarf stars with Fe/H<10 ppb. Dark blue dots are measured values, red dots are Li upper limits and light blue dots are Li and Fe upper limits. The BBN predicted range of values is shown by the red solid lines. Data from Bonifacio,(2012, 2015), Caffau,E. (2011),Frebel (2008, 2019),González Hernández (2008), Hansen (2015), Li,(2015), Matsuno, T. (2017a, 2017 b), Melendez, (2016), Nordlander, L. (2019) and, Sbordone, L. (2010). There is more than a factor of 20 difference between BBN prediction for primordial (Fe/H =0) Li abundance and observations.

While Tognelli *et al* (2020) provides a good survey of the unsuccessful attempts to resolve the Lithium problem, we can here use a paper not covered by Tognelli as an example of the problems encountered. Kusakabe and Kawasaki (2015, 2019) hypothesize that Li ions are driven out of a gravitationally contracting body by Lorentz forces generated by a ring current, thus explaining the lower-than-predicted Li abundance in EMP stars. As a result, the authors claim that a reduction of Li by as much as a factor of 4 could be explained. It should be noted that even if this were a valid deduction, it would not close the 20-fold gap between BBN predictions and observations for the lowest-Fe stars. However, Nakauchi, Omukai, & Susa, (2019) conclude that the physical conditions needed for a separation of Li ions from neutral gas do not exist in a collapsing protogalaxy because the overall ionization level would be too high.

In addition, we here point out that Kusakabe and Kawasaki also hypothesize physically impossible conditions in that their model relies on a ring current moving perpendicular to the magnetic field. With the physical conditions the authors hypothesize, $n=6x10^{-3}/cm^3$, B =30 nG, T =22 K, and ionization fraction $6.5x10^{-5}$, the ions and electrons would be highly magnetized—

that is, their gyrofrequency Ω_i, Ω_e would be much higher than their collision frequency $1/\tau_i$, $1/\tau_e$. Using standard formulae (Huba, 2013), we can calculate that for these conditions,

1) $\Omega_e = 5.3$ /s $\Omega_i = 2.9 \times 10^{-3}$ /s
   $1/\tau_e = 2.7 \times 10^{-7}$/s $1/\tau_i = 2.7 \times 10^{-9}$/s
   $\Omega_e\tau_e = 2.0 \times 10^{7}$ $\Omega_i\tau_i = 1.1 \times 10^{6}$

In such conditions, the electrical conductivity—that is, the ratio of current density to electric field—is far less for currents perpendicular to the magnetic field than for those parallel to the field. This is not due to large differences in the rate of energy loss in the different directions. It is instead due to the fact that in the field-parallel direction the electrons or ions travel between collisions a distance equal to the mean free path, L, while in the field-perpendicular direction they can only travel between collisions a distance equal to the gyroradius, r_g. Since $L/r_g = \Omega_e\tau_e$, for $\Omega_e\tau_e >> 1$, there is a large difference in conductivity between the parallel and perpendicular directions. As derived in detail in Balescu, 1988, (or see, for example, Kotelnikov, 2012) the conductivity for $\Omega_e\tau_e >> 1$ is a tensor, not a scalar, and the ratio of conductivities $\sigma_{perp}/\sigma_{parr} \sim (\Omega_e\tau_e)^{-2}$.

For the conditions considered by Kusakabe and Kawasaki with $\Omega_e\tau_e$ and $\Omega_i\tau_I$ as calculated in eq. (1), $\sigma_{perp}/\sigma_{parr} = 2.5 \times 10^{-15}$ for electrons and $= 8.3 \times 10^{-13}$ for ions. Thus, only field-parallel currents would exist, not the field-perpendicular current unphysically hypothesized by Kusakabe and Kawasaki. As is well-known on the basis of analysis, as well as on the basis of laboratory, space and astrophysical observations, (Lerner, 2021b; Alfven,1981; Fiege & Pudritz, 2000) such field-aligned currents produce a pinch effect in which ions are drawn *inwards* towards the highest-current and highest-field regions. Thus, any net drift of Li ions would be in the opposite direction to that hypothesized by Kusakabe and Kawasaki. In this example, as in other such papers, there is no successful prediction of the actual Li abundances.

We can summarize this decades-long comparison by plotting the ^{4}He and ^{7}Li observations as a deviation, in standard deviations, from BBN predictions against year. As seen in Fig. 4, both sets of observations show an accelerating deviation from predictions, with He at more than 10σ and Li at more than 45 σ. This is a deviation which has long since passed any possible reconciliation and which continues to worsen at present. Of the three light isotopes whose abundance is predicted by Big Bang nucleosyntheses, only D is in accord with predictions at 2.5×10^{-5}.

As shown in this chronological analysis, it is unquestionable that over a period of decades the actual published predictions of Big Bang nucleosynthesis, which are deduced from the hypothesis of a hot, dense origin to an expanding universe, *have been totally contradicted by subsequent observations.* This contradiction has been evident in the literature of at least the past 15 years.

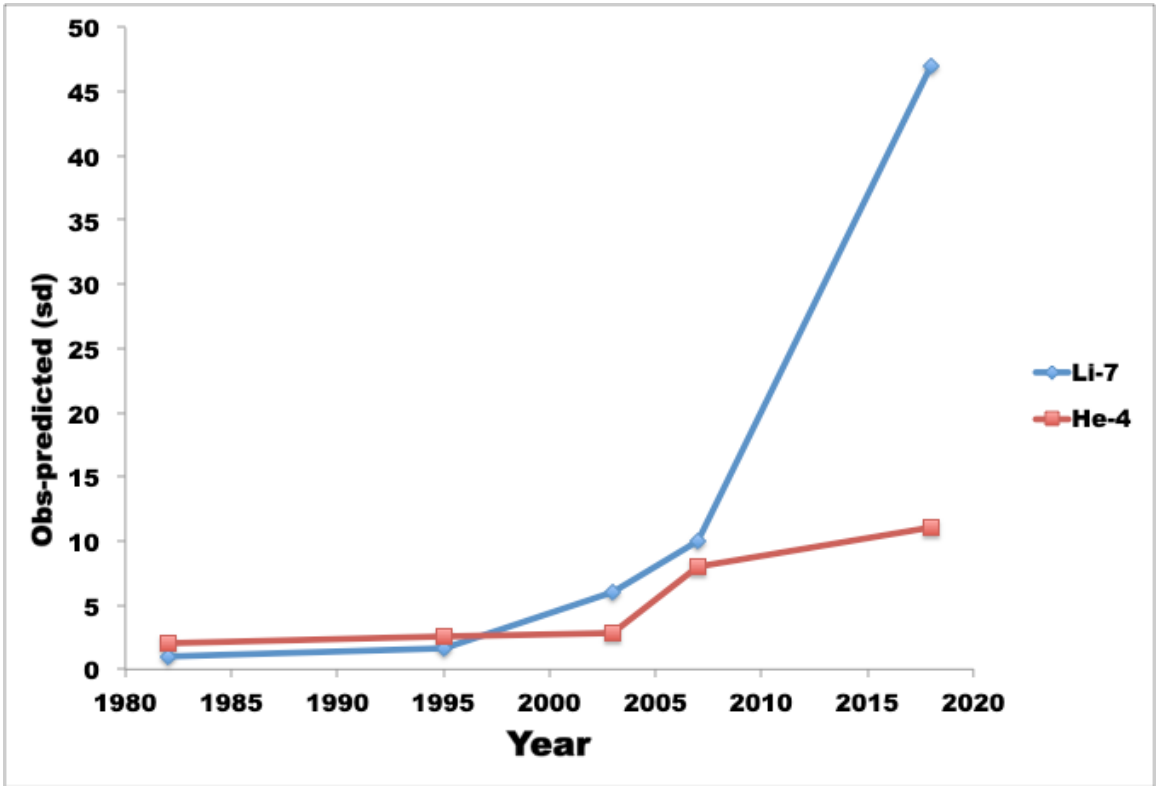

Figure 4. Difference between BBN predictions and observations in standard deviations vs year of publication of observations. The divergence has increased at an accelerating pace and has falsified the predictions decisively since at least 2007.

3. Non-Big Bang predictions for light element abundances

Efforts to explain and predict light element abundances on the basis of non-Big-Bang physical processes occurring in galaxies have been far more successful than those based on the Big Bang hypothesis. As early as 1969, only two years after Wagoner et al's Big Bang predictions, Ramaty & Lingenfelter (1969) showed that deuterium could be produced, and indeed was being produced, by cosmic rays. Ramaty pointed out a set of several reactions, notably p+p-> d+ π and p+He4->p+n+d + π that could explain the very high abundance of D in cosmic rays, around 1/6 that of ^{4}He. In 1971 Meneguzzi *et al* (Meneguzzi, Audouze &Reeves, 1971) showed that ^{7}Li, as well as boron and beryllium, could also be produced entirely by cosmic rays.

However, the first paper to explicitly propose a purely galactic origin for all the light elements was by Audouze & Silk (1983). In this paper and an elaboration (Audouze, Lindley & Silk, 1985), they pointed out that the observed amount of ^{4}He could be produced in the early stages of galaxy formation, when star production was far more rapid than in the present Milky Way. Similarly, a much larger production of cosmic rays in early galaxies could, they calculated, lead to the observed amount of D though the α+^{4}He ->^{3}He +d reaction.

Also, in 1985, Walker *et al* (1985) made the first quantitative predictions of light element abundance based on the cosmic ray hypothesis. They assumed that the ^{4}He and CNO abundances are those of the present-day interstellar medium (ISM) and that the CR production and propagation are those at present, with an accumulation time of 10 Gy. This simple model gave predictions that were a good fit to present-day observed abundances of ^{6}Li, ^{9}Be, ^{10}B and ^{11}B. The ^{7}Li /H prediction of 10^{-10} was a significant underestimate for present-day abundance, but was a good fit to the Spite-plateau, discovered 3 years earlier. The authors pointed out that another mechanism was required for additional present-day ^{7}Li but that if the Spite plateau was accepted as the primordial value, the cosmic-ray contribution would produce a conflict with the BBN predictions, driving the BBN contribution too low.

The present author elaborated (Lerner, 1988, 1989) a galactic model for the production of all the light elements, derived from basic plasma physics phenomena that have been well-studied in the laboratory and within the solar system. The model led to a prediction of ^{4}He in the range of 0.21 to 0.25 by mass and of carbon and oxygen by number relative to H of 3.5×10^{-4} and 9×10^{-4}, respectively, in agreement with observation. Deuterium, produced by the p+p->d+ π reaction was predicted to be 2×10^{-5}. ^{6}Li, ^{9}Be, and ^{10}B were predicted in the correct amounts through cosmic ray production, with additional ^{7}Li and ^{11}B produced in later galactic history through thermonuclear processes.

So, by the end of the 1980's there were actually two alternative explanations for the light element abundances, one based on a hot Big Bang and the other on thermonuclear and cosmic ray process during galactic evolution. A key question was whether Be and B, which were not predicted by BBN, were present in metal-poor, early stars. In 1991, ^{9}Be was first detected in a VMP star, (Gilmore, Edvardsson and Nissen, 1991) implying that at least some of the ^{7}Li in VMP stars must also have come from CR production.

The implications of these and further discoveries of Be in three more VMP stars (Ryan *et al*, 1992) were spelled out by Steigman and Walker (1992). They pointed out that while Be and B require collisions with CNO nuclei, Li can be produced by alpha-alpha collisions. Thus in the early galaxy, with low CNO abundances, as reflected in VMP stars, the ratio of Li production to Be and B production was very high, due to the large ratio of He to CNO abundance. They calculated that as much as half of the Spite plateau's Li abundance could be accounted for by CR production, based on observed Be abundances in early stars. This would push the ^{7}Li "primordial" abundance below that allowed by BBN predictions. The authors also emphasized that this calculation was a lower bound on the CR production of ^{7}Li. Ryan *et al* pointed out that using this same analysis on individual stars led to the conclusion that in at least one case, HD 76932 all of the Li could be accounted for by CR production.

Interest in CR production of light elements was renewed with the reported discovery, later disputed, of ^{6}Li in metal-poor stars. In 2004 Fields and Prodonovic (2004) pointed out that the production of the solar level of ^{6}Li, which is not predicted to be produced by BBN, would require large amounts of CR, which in turn would produce pions and thus observable gamma rays. They calculated a total time-integrated CR density for energy>100 MeV of $>10^{-14}$/cc, assuming that all ^{6}Li had been produced by CR with the current abundance of ^{4}He. This CR density would, they calculated, produce at least twice the observed gamma-ray background. An

unstated assumption in the work is that the CR were produced at sufficiently low density that all gamma-rays could escape to be observed.

More recently, the discovery in 2012 of ^{6}Li and ^{7}Li in the ISM of the Small Magellenic Cloud (Howk, *et al*, 2012) allowed Ciprijanovic (2016) to repeat the calculations with similar conclusions, that a level of CR production 600 times higher than that observed at present in the SMC was needed to explain the abundance of ^{6}Li, which was measured at $6.2x10^{-11}$. The author did not note, but the same CR production would inevitably lead to the production of ^{7}Li at an abundance of $1.2x10^{-10}$, or exactly that of the Spite plateau.

The galactic models of light element production such as Lerner's predicted a pre-galactic abundance of zero for all elements other than H. The observations of the past decade that show Li abundance declining towards zero with declining Fe/H seen in Fig. 3 confirm the predictions of GOLE just as they contradict those of BBN. As shown in the next section, a more comprehensive comparisons of GOLE predictions with observation provides more confirmation for with recent data for hypotheses published nearly 40 years ago.

4. Comparison of Galactic Origin of Light Elements Model with Observations

Since there have been no overall comparisons between the predictions of the galactic model of light element production in the last 30 years, it is certainly timely to do this comparison here. We here compare the predictions made by the overall model elaborated by the present author in 1988-89 (Lerner, 1988,1989). At the same time, we re-calculate those predictions using more recent data on stellar properties, allowing a better quantification of the uncertainties that remain in the model.

We first briefly summarize the main features of the earlier model, described in detail in Lerner (1989, 1986). This model starts from the central role played by the plasma filamentation instability in generating inhomogeneities in plasma at all scales from laboratory to astrophysical. Such filamentation, this earlier work shows on both theoretical and observational grounds, produce plasma vortex filaments with characteristics ion velocities of $(m/M)^{3/4}c$, where m is the mass of the electron, M the mass of the ions (in astrophysical cases, protons). This produces a hot plasma component with a characteristic ion temperature of 6 keV.

The concentration of plasma in the filaments can produce masses that can contract further gravitationally, but only if the plasmas are collisional—that is, if the mean free path is less than the radius of the filaments. Otherwise, ions in the plasma simply orbit each other without exchanging energy as is needed for condensation. Since the mean free path is simply a function of density and ion velocity or T, a constant T of 6 keV sets a relationship $nr > 1x\ 10^{19}/cm^{2}$ between plasma density n and vortex radius r. Since gravitational condensation occurs at these scales, we can restate this as a relationship between the mass M of an object that condenses from the plasma and the initial plasma density in the vortex, or $M=1.8\ n^{-2}$, where M is in M_s and n is in cm^{-3}. This relationship means that, at any given density, stars forming have a given mean mass, which decreases with increasing density. Thus, during the contraction of a galaxy, larger stars form earlier in a quantitatively predictable sequence.

Filaments moving at supersonic velocity through the contracting plasma generate shock waves that spread through the plasma. These shock wave in turn set in motion star formation. At densities $n< 0.4$ /cm^3, where stars with $M>12$ M_s form, the shock wave spreads away from the plane of rotation only until the stars begin to explode as supernovae, disrupting the shock waves. The most massive stars with $M>12$ M_s which become core-collapse SNII supernovae are thus formed in a relatively thin disk. The supernovae, in the conditions of an initially pure H cloud, by their explosions, limit the volume for the production of similarly-massive stars.

In contrast, at $n> 0.4$ /cm^3, where stars $M<12$ M_s form, supernova do not occur and the shockwaves spread away from the contracting plasma cloud's equator to the entire bulk of the galaxy. The bulk of the plasma is thus processed only through these intermediate mass stars (IMS), with masses from 4-12 M_s . Because the volume in which $M>12$ M_s stars form is much smaller than the volume of the entire cloud, the model therefore predicted that the number of supernovae would be reduced by more than a factor of 10 compared with the intermediate mass stars.

The derivation of the quantitative predictions is detailed in Lerner 1988 and summarized in Lerner 1989. We here just present the results of that derivation, eq.(2) of Lerner 1989, showing that the ratio $\mathcal{R}$ of the height of the volume that produces $M>12$ M_s and thus supernovae is:

2) $\mathcal{R} = V_a L_t / R_m = 1.43\ (M/M_s)^{-1.25}$

, where V_a is the Alfven velocity in the local plasma in cm/s, L_t is the lifetime in s of the stars of mass M and R_m is the radius in cm of proto-galactic plasma cloud. $\mathcal{R}$ ranges from 4.5×10^{-3} for $M = 100$ M_s to 6.4×10^{-2} for $M = 12$ M_s, thus predicting the strong reduction of the number of supernovae relative to IMS stars with $M<12$ M_s.

The model calculations indicated galaxy formation would take about 200 My during which the luminosity, dominated by the IMS, would exceed about 100 L*/M*. This initial intense period of energy generation would lead to the production of the "primordial" ^{4}He observed in a second generation of stars and in the ISM.

The predicted distribution of stellar mass for a young galaxy is very different than that observed for mature galaxies like the Milky Way, with far more IMS, and far fewer SN. The conditions in forming galaxies are also far different than those in mature galaxies. Galaxies forming from pre-stellar plasma can be expected to have relatively simple geometry—in our models consisting of filamentary currents, and resulting shock waves. Mature galaxies, in contrast, are observed to have far more complex fractal geometries, as well as higher mean plasma densities. There is general agreement among stellar evolution models that SN produce tens to hundreds of times more C and O per unit mass than do IMS. Thus, the ratio of C and O to He production is also different, with the predicted C and O abundances, as noted above, being 3.5×10^{-4} and 9×10^{-4} by number, not much higher values.

The model predicts that the period of intense star-formation, which involves several generations of IMS stars, ends when the continued contraction of the forming galaxy perpendicular to its plane of rotation compresses the bulk of the cloud into the disk region, where the SNII explosions have already begun to create the complex fractal structures which disrupt the filamentary currents' shock waves. The model calculations indicate that by the time the $4M_s$ stars end their ~ 200My lives and recycle part of their material back into the ISM, the galactic compression into the disk is complete and therefore stars with $M<4M_s$ are not formed in large numbers during the intense period.

The model also excluded any contribution from SNIa supernovae, which are assumed to originate in binary stars with lower-mass progenitors. This exclusion is appropriate, as observations show that even "prompt" SNIa are delayed by 200-500 My after star-formation, (Raksin et al, 2009) putting any contributions they make after the 200 My galaxy-formation period described by the GOLE model. The same observations indicate that SNIa progenitors typically have $M<3M_s$ and thus in this model would be formed at later times than the model covers and not at the same elevated rate as during the intense period.

The model in both its original 1988 version and as updated in this paper predicts only the mean stellar mass formed at a given time in the galactic formation process. The model does not attempt to derive a complete distribution of stellar abundance vs stellar mass for each time, instead assuming that all stars formed at a given time have the predicted mean stellar mass. Deriving a more realistic distribution as a function of time will require significantly more detailed simulation, and is work for future iterations of the model, as are comparisons of such predicted distributions with observations of the characteristics of stars with sufficiently low mass to survive from the earliest phases of galactic evolution.

Observations have confirmed some of the most important predictions of the model. Ultra-luminous infrared galaxies (ULIRGs) have been observed to have luminosity to mass ratios just in the range of 100 L_s/M_s, as predicted (e.g. Eser et al, 2014). These galaxies are generally the product of galaxy collisions and are thus dynamically broadly similar to the initial formation of a galaxy from converging plasma masses. Given typical collision velocities of 200-300 km/s and typical large galaxy radii of 10 kpc, collision times of ~200 My are expected. In addition, such starburst galaxies have recently been shown to be producing mainly massive stars, $M>8M_s$. (Brown and Wilson, 2019). Thus, observed ULIRGS produce similar conditions to those predicted by the GOLE model for galaxy formation.

Such high L/M ratios extending over 200My must in turn lead to the production of about the amount of ^{4}He observed in existing galaxies. Roughly, the sun will convert about 12% of its H to He in 10Gy, so about twice that proportion of He is produced in 0.2Gy with a specific luminosity 100 times that of the sun. A more detailed model in Lerner (1986) predicted a range of ^{4}He abundance from 0.21 to 0.24, for a range of galactic conditions, not the single ultra-precise prediction of the BBN. This range is entirely consistent with the range of values of 0.216 -0.23 observed in the past 30 years, as described in the previous section.

In addition, observations of such ULIRGS confirm that the production of large amounts of He in young galaxies, which must have occurred given their energy production, does not lead to much

larger than solar values of C and O. For example, spectroscopic measurements of 19 ULIRGS showed a range of 4-8x10^{-4} for O/H (Pereira-Santaella, et al 2017), close to the 1989 GOLE prediction of 9x10^{-4}. This is observational confirmation that galaxies in the early stage of formation, when they are producing energy and He at a high rate, must have far fewer SN relative to IMS than mature galaxies. The mass ratio of O/He production is only around 1%, compared to around 8% for a mature galaxy. Due to the much greater C and O production of SN than IMS, it is not possible to produce the observed low ratio of C and O to total luminosity unless the SN/IMS ratio is about a factor of 10 lower than that for mature galaxies like the Milky Way, as predicted by the GOLE model.

Unlike the BBN predictions, the galactic light element theory hypothesized that the galaxy formation started from a H plasma, and therefore predicted that some of the oldest stars would have He abundance much below present levels, as actually observed by Casagrande and Portinari (Casagrande *et al*, 2007 and Portinari *et al*, 2010).

As well, the initial 1989 D predictions of 2x10^{-5} remain validated by current quasar observations of 2.5 x10^{-5}.

Thus, unlike the case of BBN, the GOLE predictions, published long before the most sensitive observations, remain in accord with those observations and are contradicted by none.

4.1 Generation of C and O in the disk

In the present work, we want to revisit the theoretical calculations in Lerner (1989) in light of the most recent observations and calculations of stellar evolution to see if the earlier predictions still are valid, to extend the predictions to more observed correlations of abundances, and to better determine the uncertainties remaining. We first look at the original predictions for C and O production in the thin disk where SN are hypothesized to occur and see if the calculations are altered by more recent modeling of SN C and O yield.

There is a fairly wide range of theoretical yields of C and O for SN of a given initial mass. Thus, for a 60 M_s SN, Takahashi *et al* (2014) predict a yield of only 0.4% O by mass, while for the same mass SN, Marassi *et al* (2019) predict as high as 2.5% O. For a 12 M_s SN, the smallest in the range, Takahashi *et al* calculate 0.8% O and Marassi *et al* calculate 12.5%, more than an order of magnitude larger. However, most of this variation can be attributed to differences in the initial conditions, such as initial metallicity and rotation, the same variations that occur in the real SN population. Thus, Marassi shows observed Fe yield that vary for SN of the same initial mass over a range of nearly two orders of magnitude.

These large natural variations in individual SN, reflected in the models, average out to much smaller variations in populations of SN. For example, the SN models used in Lerner 1989 were approximated with an O yield mass fraction of 2.5 x10^{-3} M/M_s, (where M is the mass of the SN progenitor star) while in the Marassi model for rotating SN with initial metallicity 10^{-3} the solar value can be approximated by O yield mass fraction of $1.5/(M/M_s)$, which is the opposite dependency on stellar mass from that in Lerner. Yet if we integrate O yield over the SN mass distribution hypothesized in Lerner 1989, we find the Marassi values produce an O mass fraction

at the end of the 200 My formation period of $6x10^{-3}$, a bit less than half that with the original model, based on Arnett (1978). The use of a variety of models confirm that O and C predicted yields only vary within a factor of about two, with O mass fractions tending to be lower using more recent models and C mass fractions being about the same in older and more recent models.

Based on these new calculations, we can modify the predictions of the 1989 model for C and O production within the disk to the range of 2.5 – 5 x 10^{-4} for C and 4.5-9 x 10^{-4} for O. This is in good agreement with observations, as noted above, of ULIRGS of 4-8 x 10^{-4} for O.

There is an additional theoretical uncertainty in that GOLE hypothesizes the earliest SN in the disk are initially pure H. No modeling has been done for stars that originate with either pure H or with He abundance below around 20% by mass. This is a subject for future work.

4.2 Helium abundance

Next, we turn to the model of the bulk of the forming galaxy, outside of the disk where the model produces IMS, but no SN. This region of the forming galaxy, not the thin disk, is what is considered in sections 4.2-4.5. In Lerner 1989, it was assumed that the IMS produced no C or O. However, to compare model predictions with observations of low metallicity stars, we need a more detailed model, which does include the relatively small amounts of C and O produced by IMS. We do this by creating a homogenous model of an early galaxy, with the evolution of stars starting at a mass of 12 M_s and proceeding continuously through smaller mass stars formed from the matter processed through the earlier generations. In contrast to the earlier work, which assumed discrete generations, we here assume that the average mass varies as a power function of time, thus smoothing the evolution. This produces an analytically simple model, but one that generates very similar predictions to the original discrete one.

We first recalculate He production. In the mass range 4-12 M_s, luminosity $L \sim M^{3.6}$ (Eker, 2018) and lifetime, $L_t \sim M^{-1.8}$, so we model luminosity per unit mass as $L' \sim t^{-1.44}$. To calculate the amount of He produced, we need to know how the efficiency of returning He to the ISM varies with M. In the original 1989 model a dependency of $He/H \sim M^{1.38}$ was assumed based on theoretical calculations (Audouze & Tinsley 1976). Unfortunately, theoretical calculations of the late evolution of intermediate mass stars still have wide uncertainties, for the lower end of this mass range, resulting in calculated He yields for M=4 M_s stars that vary over a range of more than a factor of two. To cover this uncertainty, we model the efficiency of He emission to the IGM as a power function of mass, with the exponent in the range of 1.0-1.4. This leads to a range of He yield to the ISM of 4%-2.7% of the mass of the M=4 M_s stars, with the M=12M_s stars fixed at 12% He yield.

Within this range of parameters, the resulting ISM helium mass fraction at the end of the galaxy-formation process is 0.248+-0.009. This is close to, but 3% higher than the 1989 calculations, and still entirely consistent with the observed range.

Of course, the key difference with the BBH predictions is that in the GOLE model this range is not a minimum, but rather the end point of the period of galaxy formation in an individual galaxy. The pre-galactic He/H value with no Big Bang is hypothesized to be zero, so the much

lower He abundance values observed in recent years remain entirely compatible with the GOLE model. In addition, the model also naturally predicts the rarity of stars with He/H<0.11, as the first generation of stars produces this much He, and less massive stars that survive to the present in our galaxy are unlikely to form before the end of this first generation. This is due both to the high mean mass of the first generation of 12 M_s and to the greater homogeneity of the plasma prior to the large stellar winds occurring at the end of the first generation. So we find that the GOLE model is still consistent with He abundance observations.

We point out here that the energy generated by the production of the observed amount of helium is close to the amount contained in the cosmic microwave background (CMB), an equivalence that has been noted for decades, including in the original formulation of the GOLE model (Lerner, 1988). Taking the GOLE-model prediction of thermonuclear energy release of 4 Mev/H and the known CMB energy density of 0.26eV/cm^3, a total H density of 6.6 x10^{-8}/cm^3 is required. By comparison, the theoretical baryonic density predicted by the current BB model is 2.5 x 10^{-7}/cm^3 and the observed mass density in stars in the local universe is in the range of 1.5-3 x10^{-8}/cm^3 (Gallazzi et al, 2008). Since the total mass of H involved in stellar formation must exceed the mass currently in stars, an actual H density of 6.6 x10^{-8}/cm^3 is entirely consistent with observations. Such an energy release will thus produce the observed 2.7 K background radiation temperature if it is thermalized to equilibrium. This is further discussed in section 8.

4.3 Deuterium

Turning to the predictions for deuterium, we have to first consider the observational evidence for the amount of CR hypothesized by the GOLE theory to produce the observed abundance of D. In the earlier papers (Lerner, 1988, 1989) the author's calculations predicted that a total CR energy of about 1-2% that of total thermonuclear energy would produce D/H in an abundance of 2 x 10^{-5}. Since the energy density of the CMB is 4.2x10^{-13} erg/cm ^{3}, and since the GOLE model hypothesizes that this is energy produced by thermonuclear reactions in stars, this calculation predicted a CR density of 4-8 x 10^{-15} erg/cm^3. There is no direct observational evidence for the mean CR density on the largest scales, since we can only directly sample CR within our own galaxy. However, since CR produce both gamma rays and neutrinos, we can use observations of these particles to obtain an indirect measure of total CR density.

At present, observations covering the whole range of neutrino energies are not available, as ground observations are masked by neutrinos generated in the atmosphere. At high energy, astrophysical neutrinos dominate. Measurements by the IceCube Collaboration (Aartsen et al,2020) give a total energy flux of neutrinos at 10 Tev energy as 0.51+-0.19 keV/cm^2 s sr. As a first approximation, if we assume the neutrinos are produced in the ISM of galaxies and in the IGM by a CR energy spectrum the same as that in the Milky Way, we can use existing modeling (Mazziotta et al, 2016) to determine that total neutrino flux would be 4.1 +-1.5 Mev/ cm^2 s sr. Neutrino energy density would then be 0.9 +-0.3 x 10^{-15} erg/cm^3. With about 40% of CR energy going to produce neutrinos, this would imply the production of a CR energy density of 2.2+_0.7 x 10^{-15} erg/cm^3, about half what was predicted in the original GOLE theory.

However, it we look at the gamma ray spectrum, we will see that the naïve assumption of production of neutrinos in the ISM and IGM can't be correct. In low-density environments, CR will produce about 50% more energy in photons than in neutrinos. But from the FermiLAT data on the EGB (Ackermann et al, 2015) GR radiation at 1 Tev is only about 0.6% of the neutrino radiation extrapolated from the 10 Tev measurement of IceCube. In the entire energy range down to the GeV level, the EGB remains a factor of about 250 below what would be produced by a CR distribution with an initial energy density of 2×10^{-15} erg/cm^3.

These puzzles can be resolved by taking into account an observed feature of CR that was overlooked in the earlier work: *most CR are trapped in magnetic fields and propagate downwards, back to the stellar surface.* Since the 1980's, observations of solar CR generation and the associated GR emissions have shown that downwards collisions of trapped CR particles with the denser layers of the solar atmosphere must significantly exceed the upwards escape of particles. Yoshimori (1990) estimated from observations that downwards moving ions exceeded upwards ones by a factor of 10-100 depending on the individual solar flare. Ackermann et al (2017), showed from multiple satellite observations of the same flares that the ions are trapped and collide with the photosphere, producing gamma rays representing only about 2% or less of the total energy of the CR particles (table 2 of Ackermann et al).

Is an attenuation of the order of 100 of GR physically reasonable for a predominantly downward-going CR distribution on stars? The attenuation of GR from downward CR is mainly due to relativistic beaming. The absorption cross section for >100 Mev photons is less than that for proton-proton interactions that generate pions, so absorption is not a major factor except for radiation generated near the stellar limb for a given observing direction. However, relativistic beaming produces a decrease in the backward-directed luminosity of $\sim ((1-\beta^2)^{1/2}/(1+\beta))^3$. From the galactic CR spectrum measured by Voyager, which is produced from a combination of massive stars and supernovae, we calculate that attenuation factor is indeed close to 100, including the unattenuated radiation from the fraction of CR that escape into the ISM and IGM. Of course, GR directed downwards into the bulk of the star are completely absorbed and not observed. In contrast, neutrino cross sections in the TeV energy range are of the order of 10^{-33} (Tev/E) cm^2 , so we can calculate that 85% of even 1000 TeV neutrinos escape.

It is clear that even stars the mass of the sun have magnetic fields that are adequate to confine CR up to high energies. Charged particles can be confined so long as their gyroradius is less than the radial extent of the magnetic field. For highly relativistic velocities, the proton gyroradius is:

3) $r = 3.3 \times 10^{-3}$ E/B cm

where e is the charge of the particle, E is the particle energy in eV and B is the magnetic field strength in gauss. In a field created by a linear current I amps, particles will therefore be confined (at least for several gyro periods) if

4) E< 60 I

Since observations show that currents in solar flares are typically of the order of 50 TA, the sun can confine protons up to 3PeV, and it is reasonable to assume that more massive stars have larger currents.

We thus hypothesize that the CR particles collide with the dense surface of stars. In this calculation, we assume the same CR energy spectrum as observed by Voyager at low energy and AMS and ACE at higher energy, a spectrum that peaks around a few GeV (see, e.g. Yuan, 2019). We find that nearly 0.9 D nuclei are produced per CR proton, more than in the ISM. This is because the dominant reaction for energies <1.5 GeV produces neutrons. In a dense plasma, such neutrons are far more likely to be absorbed, producing D, than to decay back into protons, in contrast to the situation in the low-density ISM. With the mean CR energy being 1.5 GeV for the observed spectrum; a ratio of CR to total thermonuclear energy of 0.5+_0.2%, as derived from the neutrino calculation; and total thermonuclear energy of 4 MeV/H, as calculated from our model; we then get a predicted abundance of D at the end of galaxy formation of $1.4+\_0.6 \times 10^{-5}$/H of pregalactic hydrogen.

However, to compare with observed He/H in the ISM we have to account for the loss of H in the production of He and the loss of D in hot plasma at large depths in stars. The model described in section 4.2 predicts a total loss of H converted to He of 57+-2%, including He trapped in white dwarfs and other stellar remnants. Similarly, it predicts the loss of 14+-1% of D, based on the amount of He produced after the first generation of stars, since D will be destroyed in approximately the same regions where He is produced. This leads to a concentration factor for D/H in the ISM of 2.0+-0.1 and thus $D/H = 2.8 +- 1.2 \times 10^{-5}$ in the ISM at the end of galaxy formation, in agreement with the 2.2×10^{-5} predicted in 1989. The predicted range is a slight overestimate, as D is destroyed in a larger volume in stars than He is formed in. There has been no published modeling of this difference but even a doubling of D destruction would result in only a 14% reduction in predicted abundance. The new calculations are also in agreement with observations of D/H of 2.5×10^{-5}. As noted above, D/H is the one abundance that is also correctly predicted by BBH.

Thus, the addition to the GOLE hypothesis of the observation that most energetic particles are trapped near stars both resolves the discrepancy between the GR and neutrino backgrounds on the one hand, and the apparent discrepancy between the GR background and the CR energy needed to produce the observed D abundance.

4.4 Lithium

To model the production of lithium, we need to add the scaling of CR generation as a function of time or stellar mass. Unlike D production, Li production depends on the changing abundance of helium as the main production reaction is $\alpha + {}^4He \rightarrow {}^7Li + p$.

The scaling of CR generation as a function of L' is observationally uncertain, but if we assume it too is a power law, we can constrain it by assuming that the total CR energy is that calculated in the previous section. If we model the efficiency of CR production, averaged over stellar main-sequence lifetime, as a function of L',

5) $ECR/L' = a\ L'(MeV/H\ My)^{b}$

, where ECR is the energy of CR emitted in Mev/H and a and b are parameters, then for the range $1.3<b<1.65$, the range for a is $0.15<a<0.74$. For a mean CR energy of 1.3 GeV (from the previously-cited spectrum) this implies $CR/H = 1.5+-0.6x10^{-5}$ by number. For this range, the efficiency ECR/L' for the largest 12 M stars then varies within the range 0.8+-0.3%. Extrapolating (5) down to solar mass this gives a range of $2.5x10^{-6}<ECR/L'<2.5 \times 10^{-7}$. Since the observed CR energy flux that escapes the sun is about $2.5x10^{-8}$ times the total solar flux the range in b would imply a range for the sun of 10 < total CR/escaped CR <100. This range in b is thus chosen to be consistent with the observed range reported by Yoshimori and Ackermann.

It should be noted that, since the GOLE model predicts that SN do not occur in the bulk of the galaxy during formation, only in the disk, we are here not including any CR from SN, but only CR produced by IMS over the course of their lifetimes, including the period of more intense activity after stars leave the main sequence.

Using the known cross-sections for the alpha-alpha reaction (King *et al* 1975, Mercer, et al, 2001), which have about 10% experimental error, we find that 1.7R% of α-particles produce lithium nuclei, where R is the number ratio of ^{4}He to H. We assume that lithium production begins with the formation of a second generation of stars containing helium. We take this to occur ~6 My after the end of the lifetimes of the first-generation stars. This allows time for the formation of molecular clouds (Pringle, 2001). Over this range of star-formation times and the above range of $1.3<b<1.65$, we have at the end of the 200 MY model period, A(Li) = Log (Li/H) +12 = 2.4 +-0.16, in complete agreement with observations of the Spite plateau of Log (Li/H) +12 =2.36+-0.025.

Only the parameter b affects the ratio of Li to D, as both are equally affected by the total CR number. There is good agreement between the predicted range of Li/D of $1.13+-0.18x10^{-5}$ and the observed ratio of the Spite plateau to the D quasar measurements of $0.89+-0.06 \times 10^{-5}$. If we instead use the observed values of Li and D to determine the parameters a and b, we get a=0.7 and b= 1.65, showing that there exist parameters within the ranges that accord with both observed abundances.

4.5 Carbon, Boron and Beryllium

The calculations in the previous sections refer to the situation at the end of the formation of an individual galaxy. However, the GOLE model also allows the calculation of elemental abundances in the ISM at earlier times. Observational evidence for such early abundances comes from relatively rare low-mass stars ($M<M_s$) formed after the first generation in denser-than-typical environments at epochs when the mean stellar mass is much larger. These low-mass stars thus survive to the present day. To compare predictions with observations, we must look at the abundances of carbon and oxygen, and their correlations with Li, B and Be. Again, it should be noted that in this section, we are again looking at conditions in the bulk of the forming galaxy, not in the thin disk where SN occur.

Like Li, carbon is produced from the reactions of He nuclei and is similarly calculated from the combination of He abundance and total energy production rate. Again, stellar evolution models differ greatly in predicting the efficiency of carbon release to the ISM for a given M. For low-metallicity stars, models show a range a C production from 0 to $1x10^{-6}$/ H My, averaged over stellar lifetime, for stars of mass 4-9 M_s (Doherty et al, 2014; Seiss, 2010;Ventura et al, 2014). It is important to note here that these calculations lead to expected C yields over the life of the stars of at most $3x10^{-5}$ by number, about a factor of 100 smaller than the yields of SN. Given the large range in predictions and that the published models do not model different He abundances, we here model the carbon release efficiency as a constant, with the rate of carbon production per H nuclei being

6) $C(t) = c\, L' / My$

, with $1x10^{-6}$ /MeV<c<$6x10^{-6}$/MeV, and with the time of the start of carbon emission to the ISM 10-12 My after the formation of the first helium-containing stars. The range of c is selected to be consistent with the range of low-metallicity IMS models. This is the equivalent of releasing one atom of C for every 6,000- 30,000 He nuclei generated.

Assuming a constant ratio of C release to He production is an oversimplification, since there is no doubt that this process must be affected by both the mass of the star and the initial abundance of He, which affects both the time to burn H and the opacity of the star. However, modeling these two dependencies has almost no effect on the calculation here, so the simpler relationship in eq (6) is used.

Once the model predicts the amount of C produced, it can as well predict B and Be production. In both cases the dominant reaction is from the collision of protons with carbon nuclei. Using the best available reaction cross-sections (Soppera, *et al*, 2018, Fontes, 1975) and the observed spectrum of galactic cosmic rays (Cummings, *et al*, 2016), we can calculate the rate of production of these elements for a given abundance of carbon and a given number of cosmic ray particles. If we assume that all particles lose their energy to collisions or reactions in a predominantly downwards emission, we find that

7) $(^{11}B+^{10}B$ /H My) = 8.2 ± 1.6 (C/H) (CR/H My)
8) $(^{9}Be$/H My)= 0.26 ± 0.05(C/H) (CR/H My)

where (CR/H My) is the number of cosmic ray particles per hydrogen atom per My in the galaxy. In the calculation for boron, reactions with oxygen are included, assuming a ratio of O/C of 4, based on observations of low-metallicity stars.

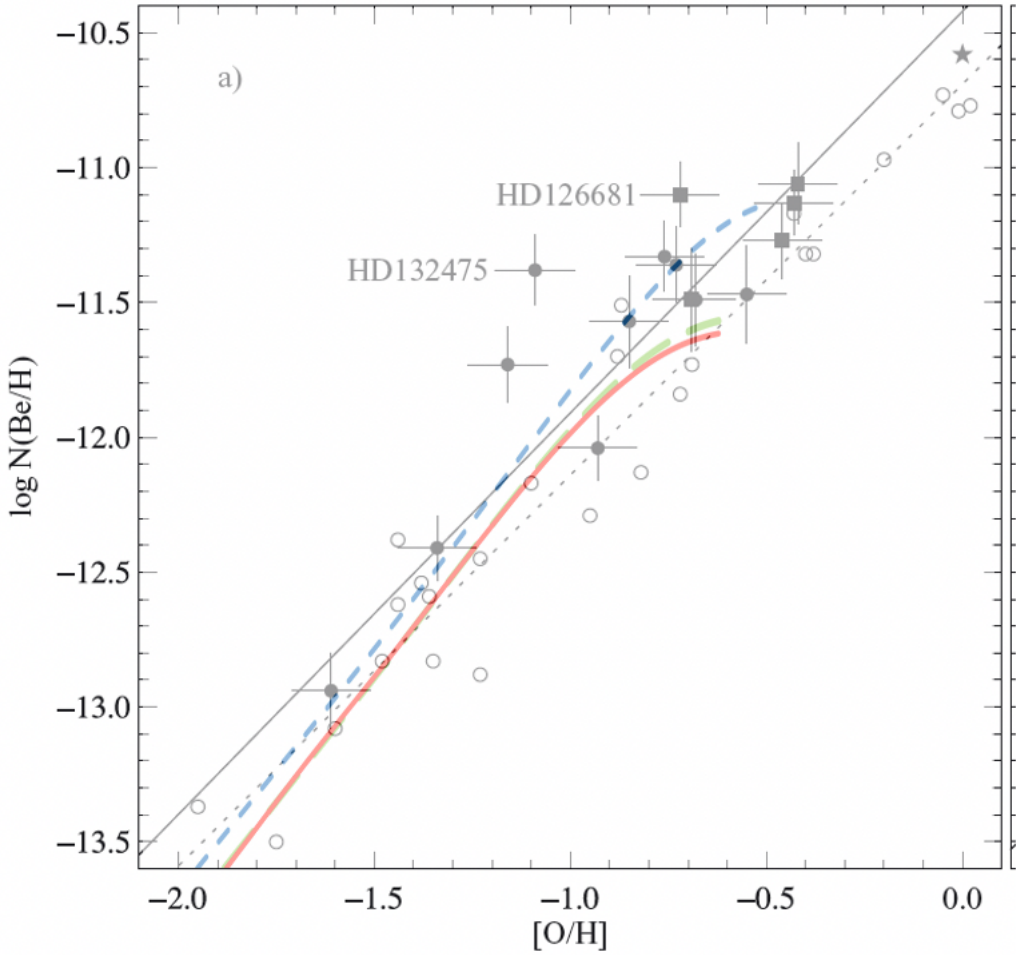

Figure 5. Data on beryllium vs. oxygen abundance (from Tan, Shi and Zhao, 2009) are well fitted by the predictions of the GOLE mode. The straight diagonal lines are fits to the solid and open data points respectively. The predictions cover the first 200My of the model galaxy. Blue short-dash line is GOLE prediction with parameters a=0.34, b=1.3, c=$6\text{x}10^{-6}$*. Red thick solid line is with a=0.65, b=1.65, c=*$4\text{x}10^{-6}$*. Green long-dash line is with a=0.42, b=1.5, c=*$4\text{x}10^{-6}$*.*

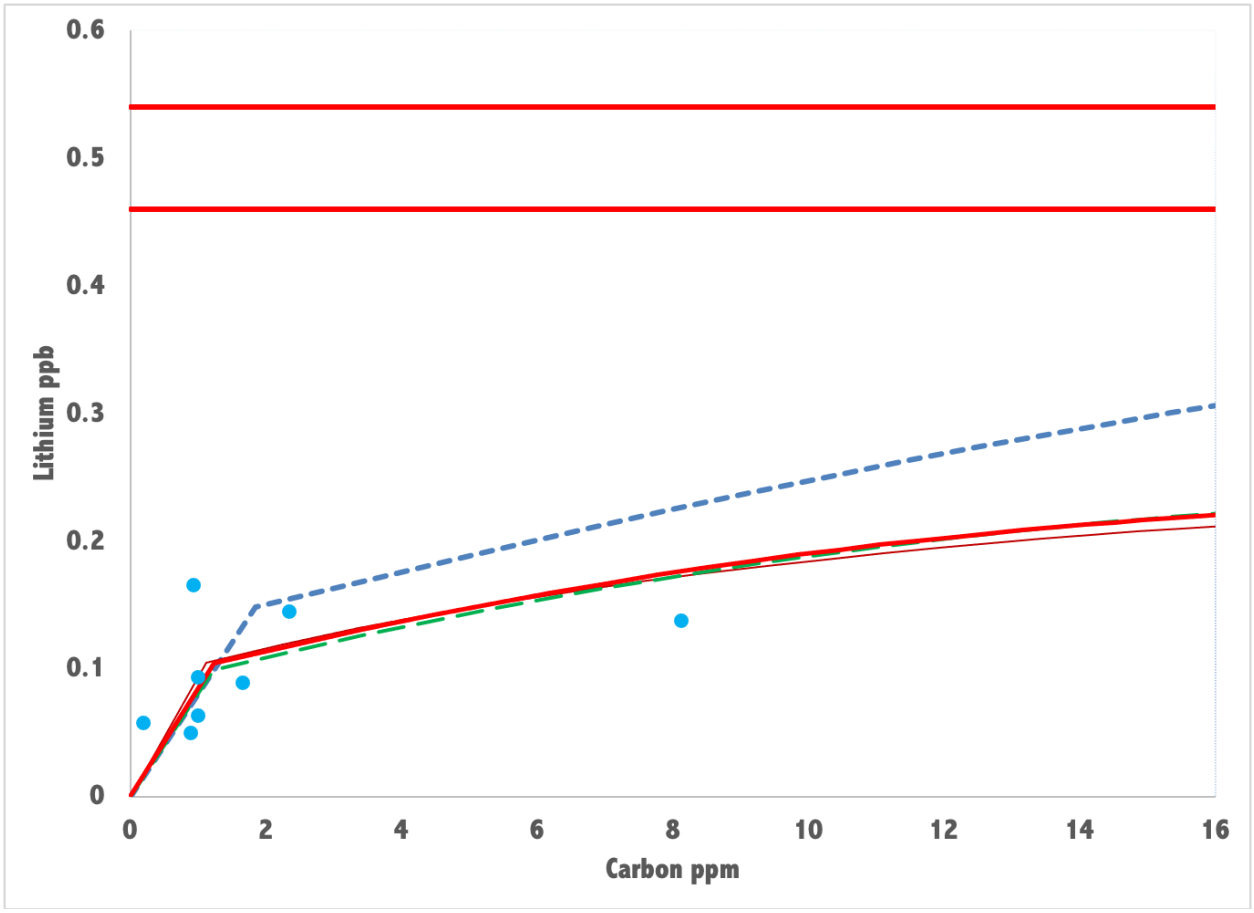

Figure 6. Lithium vs carbon abundance. Data (blue points) are from Matsuno et al, (2017) and Frebel, et al, (2019) . Solid thick, short-dash and long dash curves are GOLE predictions with the same parameters as in fig. 5. Red horizontal lines define range of BBN predictions. Thin red line uses a model with carbon efficiency dependent on both stellar mass M and initial He/H ratio. Note the insignificant difference with simpler model with constant carbon efficiency.

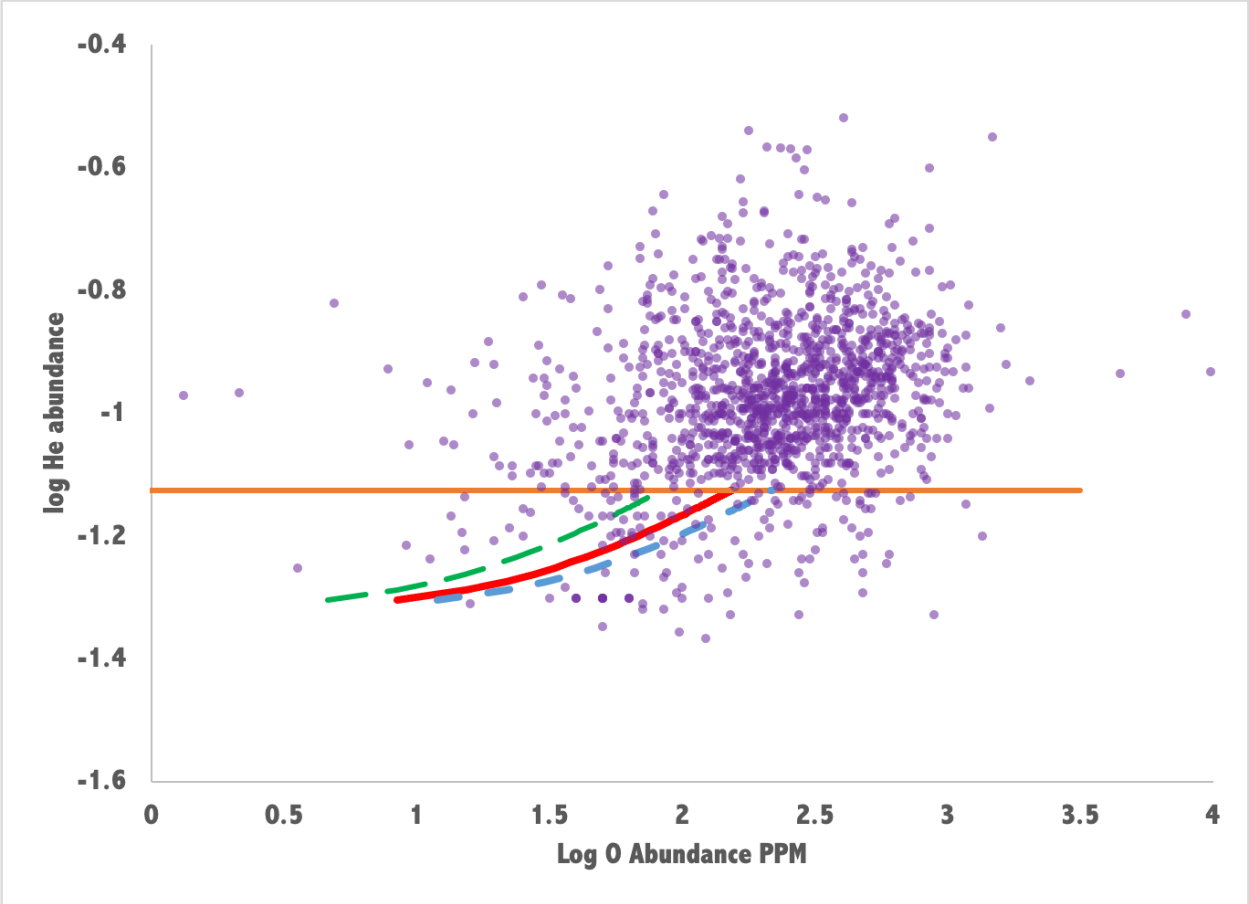

Figure 7. Log helium vs oxygen abundance spectroscopic data from Maciel, Costa, & Cavichia,2017 (dots) compared with BBN prediction for primordial objects (solid horizontal line) and GOLE predictions (curved solid and dashed lines, with parameters as in fig.5).

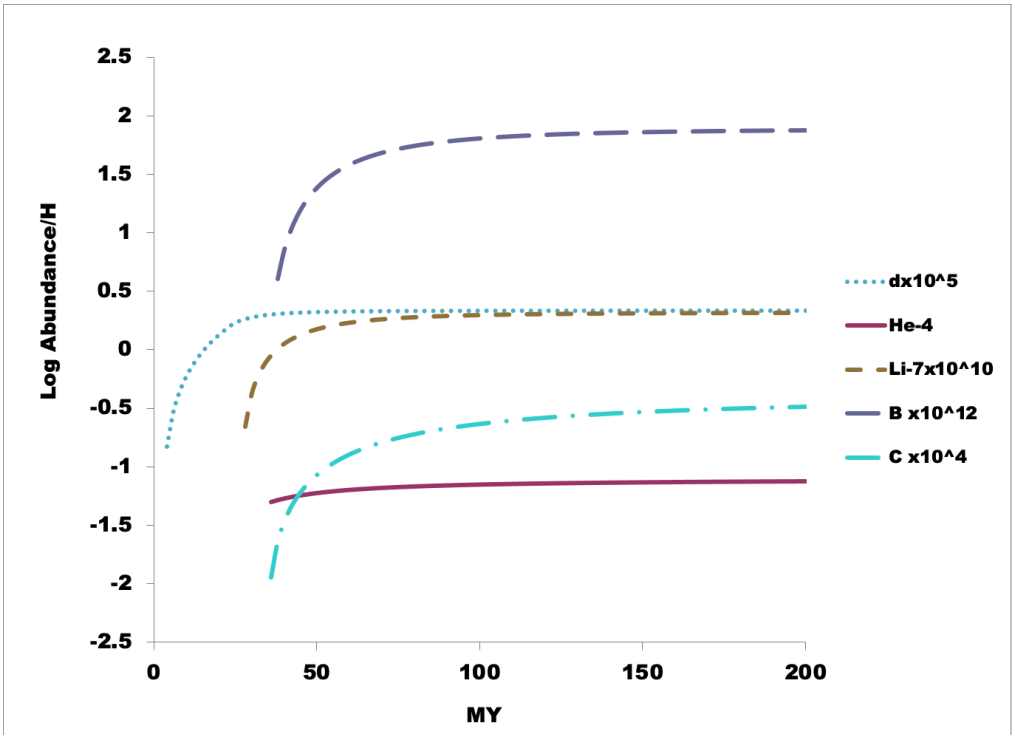

Figure 8. The log abundance of d, He, Li, B and C are plotted against time in MY in the GOLE model of the formation of a typical galaxy like the Milky Way, with no prior contribution from a Big Bang. Parameters are the same as for solid line in Fig.5.

To compare predictions for B and Be with observations which link these abundances with O abundance, we can use the observed correlation of C with O abundance in low-metallicity stars Nissen et al (2014) of

9) $(O/H) = (C/H)^{0.864} + 0.064$

If we vary the parameters a, b, and c from eqs. (5) and (6) within the specified ranges, we find that we can achieve a good fit to the Be vs O observations for a somewhat reduced range (1σ) of $0.34<a<0.7$ and $4\times10^{-6}<c<6\times10^{-6}$ with the full range of b (Fig. 5).

It is important to note that the Be-O data can be used to constrain the CR parameters of eq.(5) *independently* of the neutrino data or of any of the theoretical hypotheses of section 4.2. The range of CR parameters a and b obtained by fitting the Be-O data can then be used to predict a total CR production of $1.7\pm0.4 \times10^{-5}$/H, an ISM D abundance of $2.3\pm0.6 \times 10^{-5}$/H and a lithium abundance A(Li) = 2.44+-0.12. This is confirmation of the physical reasonableness of the parameter ranges for a and b, as they can be obtained from the Be-O data, only assuming the form of eqs. 4 and 5. This is particularly significant, since BBN predicts negligible production of Be and O, so there is no question that Be and O are only produced by the CR and thermonuclear mechanisms hypothesized in the GOLE model. *If there are enough CR to produce the observed Be-O correlation, there are as well enough to produce the observed amounts of both D and Li,*

leaving no room at all for any production by BBN. A single consistent level of CR production leads to correct predictions for Li, D, Be, and B abundance as well as for neutrino flux.

As predicted by eqs (7) and (8) the abundance of B is consistently close to 30 times the abundance of Be at all metallicities. This can be seen, for example, by comparing Fig 1-3 of Sun (2015) with Fig 7 of Tan(2009). Thus a fit to the Be data is also a fit to the B data.

Using the same parameters, the model also fits the relatively sparse data for Li correlation with C abundance (Fig.6). Here, it is clear that the parameters predicting the solid lines in both figures provide a better fit to the Li-C data. These parameters, a=0.7, b=1.65, c=$4x10^{-6}$, predict D/H = $2.5\ x10^{-5}$ and A(Li) = 2.38 at the end of galaxy formation, in excellent agreement with observations.

Included in Fig. 6 is a line showing predictions for a more complex model of C production which includes a power-law dependency on both stellar mass an initial He/H ratio. As can be seen, the additional parameters produce an insignificant change in predictions. This is because the two effects tend to cancel out and because the key variables, the rate of CR production at a given C and O abundance, are not affected by the hypothesized dependency of C production.

With the same parameters, we compare predictions to the He vs O data in Fig.7. Here, the large scatter in the observed values hinders a precise comparison, but it is clear that the GOLE predictions are consistent with the range of observed He values, while the BBN predictions are not, being in conflict with the large number of observed values with He/H<0.075. Again, the range of parameters between the solid and long-dashed lines in Fig.7, with less C and O production, provides a better fit than the higher-production short-dashed line. The O/H abundance only reaches 1-2 x 10^{-4} by the end of the galaxy formation period in the bulk of the galaxy, prior to mixing of the ISM with the more enriched plasma of the thin disk.

The predicted curves show a plateauing of He abundance with decreasing O abundance. This is because C and O production from He can only start after the lifetime of the first generation of stars, which have produced the He from an initial pure H plasma. Since this first generation produces about a He/H mass ratio of about 0.11, as noted in section 4.2, stars even with extremely low amount of C and O, orders of magnitude less than solar, still have at least a He/H ratio of 0.11. The rate of production of C, and thus also of O, defined by eq.4 implies that the earlier the stars form, the less the abundance of C and O. So there is no lower limit on the expected abundance of C and O, but there is on He. This is the case even if first-generation stars emit small amounts of C and O, since they can do this only at the end of their lifetimes, after almost all He production has already occurred.

The overall evolution of the predicted abundances with age of a young galaxy is shown in Fig. 8, showing that D, He and Li plateau early, by around 50 My, while C and B continue to rise. The predictions of the original GOLE paper and the present papers' predictions, as well as observations, are summarized in Table 1. There is good agreement between both versions and with observations.

Table 1 Summary of GOLE Predictions and Observations

Element or Isotope	GOLE 1989	GOLE 2020	Observation
Deuterium	2.2×10^{-5}	$1.7\text{-}2.9 \times 10^{-5}$	2.5×10^{-5}
Helium	23-25%	24-26%	22-25%
Lithium	1.2×10^{-10}	$2.1\text{-}3.6 \times 10^{-10}$	$2.1\text{-}2.5 \times 10^{-10}$

Table 1. The predictions of GOLE for the end of the galaxy-formation period recalculated in this paper (GOLE 2020) column are in good agreement with both those of the original GOLE paper, Lerner, 1989, (GOLE 1989) and with observation. Each abundance is by number relative to H, except for He which is as a percent of total mass.

To summarize this section, *multiple sets of data regarding He, D, Li, Be, C and O abundances are consistent with the predictions of both early and current calculations based on the GOLE hypothesis. The GOLE hypothesis provides a far better fit to the data than BBN.*

It is of course true that the GOLE hypothesis does not make as precise predictions as BBN. That is because GOLE's predictions are based on observations of the real physical processes of stellar evolution, not on *apriori* mathematical hypotheses without observational basis, such as inflation and dark energy. Further research and observations will improve the GOOE predictions. However, the key point demonstrated in this section that GOLE is a physically plausible model consistent with all observation of stellar evolution, galactic evolution, cosmic rays, neutrinos and stellar abundances. This is empathically not true for BBN, as demonstrated in the previous section. The predictions of BBN are not wrong by small amounts but by factors that are large absolutely, not just in comparison to ultra-precise predictions. Moreover, the production of light elements by the GOLE processes—an unavoidable consequence of observed thermonuclear and CR processes—greatly aggravates the contradiction between BBN predictions and observations, since the light elements which must have been produced during galaxy formation have to be subtracted from observe abundances to arrive at a "primordial" or pre-galactic abundance.

5. Implications of GOLE and BBH for the antimatter problem

The hypothesis that the light element abundance is due to processes occurring in developing galaxies assumes the absence of a hot, dense, Big-Bang phase of universal evolution, which, as is shown in the earlier sections, would produce the wrong amounts of light elements. Obviously, this hypothesis has implications for several data sets, other than those involving light element abundances alone. In this and the subsequent sections of this paper, I examine these implications to compare the validity of GOLE and Big Bang hypotheses. We here use GOLE to refer to the basic hypothesis that the Big Bang did *not* happen, while we use BBH to refer to the hypothesis that the Big Bang *did* happen.

As is well-known, the so-called "antimatter problem" causes the Big Bang to predict matter densities that are far less than those observed. As it cools, any hot dense phase of universal evolution will lead to the annihilation of most protons and antiprotons that were produced at higher temperatures. Such annihilation would limit the density at the time that the cosmic temperature fell below 1 GeV and the production of proton-antiproton pairs from photons was no longer possible. The density limit would be of the order of

$$10)\ n_c = (tc\sigma)^{-1}$$

where t is the "age of the universe" at this time, c is the speed of light and σ is the annihilation cross section of protons and antiprotons at 1 GeV energy. Since t=2.2 microsecond and $\sigma = 5x10^{-26}$ cm^2, n = $2.8x10^{20}$/cm ^{3}. Since this density would exist at a z=3.6 x 10^{12}, the current predicted density would be around 6 x 10^{-18}/cm 3, around 10^{11} times less than observed.

This huge gap between prediction and observation has been long known, for example (Chiu, 1966). Although the exact magnitude of the gap has been calculated differently, all sources put it at between a factor of 10^9 and 10^{11}. While this gap between prediction and observation, like that for the light elements, is certainly evidence against the validity of the Big Bang hypothesis, it has not been treated that way in the vast majority of papers. Instead, it has been attributed to an unknown process that produced baryon number non-conservation---more baryons than anti-baryons. Such processes have never been observed in any experiments on earth.

Any such processes would necessarily imply a finite lifetime for the proton. Indeed, a lifetime of around 10^{30} years was originally predicted by Georgi, Quinn and Weinberg, (1974) as a necessary condition for resolving the antimatter problem. As experiments ruled out longer and longer lifetimes, these Grand Unified Theories (GUTs) were modified to predict longer lifetimes (Lopez, J. L., Nanopoulos, D. V. & Pois 1992) However, to date observations have ruled out a lifetime even 10^4 times larger, excluding all these theories (Tanaka *et al*, 2020). There is no experimental evidence of a finite lifetime for the proton. But the lack of such a finite lifetime would rule out the baryon number non-conservation needed to overcome the 10^{11}-fold gap between Big Bang baryon density predictions and observations. So this massive contradiction of prediction and observation still exits.

By contrast, with the GOLE hypothesis that excludes a phase of high density and high temperature, no antimatter problem exists. First, a universe that never went through a period of high temperature and high density, and thus massive pair production and annihilation, would

have no necessity to have a matter-antimatter number symmetry. It would be entirely consistent with present observations that the universe has always been matter-predominant.

Second, even if future observation turn up evidence of distant antimatter, Alfven and Klein (Alfven and Klein, 1962) showed 60 years ago that a matter-antimatter symmetric plasma at low density and temperature would naturally separate out into pure matter and pure antimatter regions. In the present-day universe, regions dominated by matter and antimatter would be separated from each other by magnetized zones that are so thin that the radiation from them would be at very low levels (Lehnert, 1978). For example, from Lehnert's formula (8), for conditions typical of the intergalactic medium ($n= 10^{-7}/cm^3$, T=100 eV) boundary zones would have typical thicknesses of the order of 0.3 AU and emit proton-antiproton annihilation radiation at a flux that is billions of times less than the observed GeV background. In *either case*, the far greater observed local abundance of matter poses no "antimatter problem" for GOLE and no contradiction between prediction and theory exists.

6. Expansion of the Universe and Surface Brightness Test

A third major difference in implications between BBH and GOLE is that a hot, dense epoch for the entire universe, not just parts of it, requires an expanding universe to arrive at the present dilute, cool state. Indeed, the BBH, although not by that name, was originally proposed as an explanation for the observed Hubble relation between redshift and distance, interpreted as an expansion of space. In contrast, GOLE hypothesizes that no expansion that could be extrapolated back to a hot dense epoch could have occurred.

Surface brightness provides a purely geometrical test of the reality of expansion. As Tolman (Tolman 1930,1934) demonstrated, in any expanding cosmology, the surface brightness (SB) of any given object is expected to decrease very rapidly with z, being proportional to $(1+z)^{-3}$, where z is the redshift and where SB is measured in AB (per unit frequency) units. (The exponent is -4 for bolometric units). By contrast, in a static (non-expanding) universe, where the redshift is due to some physical process other than expansion (e.g., light-aging), the SB is expected to be strictly constant when AB magnitudes are used.

The predictions of BBH for surface brightness of galaxies are complicated by the prediction of the theory that galaxies will change size with time. Mo, Mao and White (Mo et al, 1998) first showed that the radius of disk galaxies forming at redshift z should be a fixed fraction of the size of the dark matter halo. This in turn is proportional to $H^{-1}(z)$ for fixed virial velocity or $H^{-2/3}(z)$ for fixed mass, and somewhere in between for fixed absolute luminosity L, where

11) $H(z) = H_0[\Omega_m(1 + z)^3 + \Omega_k(1 + z)^2 + \Omega_\Lambda]^{1/2}$

, where Ω_m is the ratio of matter density to closure density, Ω_Λ is the ratio of dark energy density to closure density and Ω_k is the curvature parameter, assumed to be zero for an inflationary universe.

It was only with the release of the Hubble Ultra-Deep Field data that these predictions could be tested at high z, and subsequent data sets allowed tests with both disk and elliptical galaxies. The

present author (Lerner, 2018) showed that these size predictions based on the size-evolution, expanding-universe hypothesis are incompatible with galaxy size data for both disk and elliptical galaxies. For disks, the quantitative predictions of the Mo *et al* theory are incompatible at a 5-sigma level with size data, as is any model predicting a power-law relationship between H(z) and galaxy radius. For ellipticals, a power law of H(z) does fit the data, but only with an exponent much higher than that justified by the Mo *et al* theory.

Equally important, Lerner shows in the same paper that all three physical mechanisms proposed in the literature for the size growth of galaxies-- "puffing up" (Fan *et al*, 2008), major (Cole, *et al*, 2000) and minor mergers, (Naab, *et al*, 2009), —make predictions that are contradicted by the data, requiring either gas fractions or merger rates that are an order of magnitude greater than observations. In addition, any size evolution model for ellipticals leads to dynamical masses that, given the observed velocity dispersions, are smaller than stellar masses, *a physical impossibility*. Peralta de Arriba *et al* (Peralta de Arriba *et al* ,2015) report that, using stacked spectra to determine velocity dispersions, galaxy samples at $z>0.5$ have M_{dyn}/M_{stell} as low as 0.4, well below the physically possible limit of 1.

In contrast to failed predictions of BBH plus size evolution, the author and colleagues (Lerner, 2006, 2009, 2018; Lerner, Falomo, and Scarpa, 2014) have demonstrated that extensive SB data for both disk and elliptical galaxies is entirely compatible with a static universe where z is linearly proportional to distance for all z. (A hypothesis of the relation of distance and z in a non-expanding universe is necessary in order to convert apparent magnitudes to absolute magnitudes and thus to compare the SB of galaxies with the same absolute luminosity.) That is, the observed SB is independent of z.

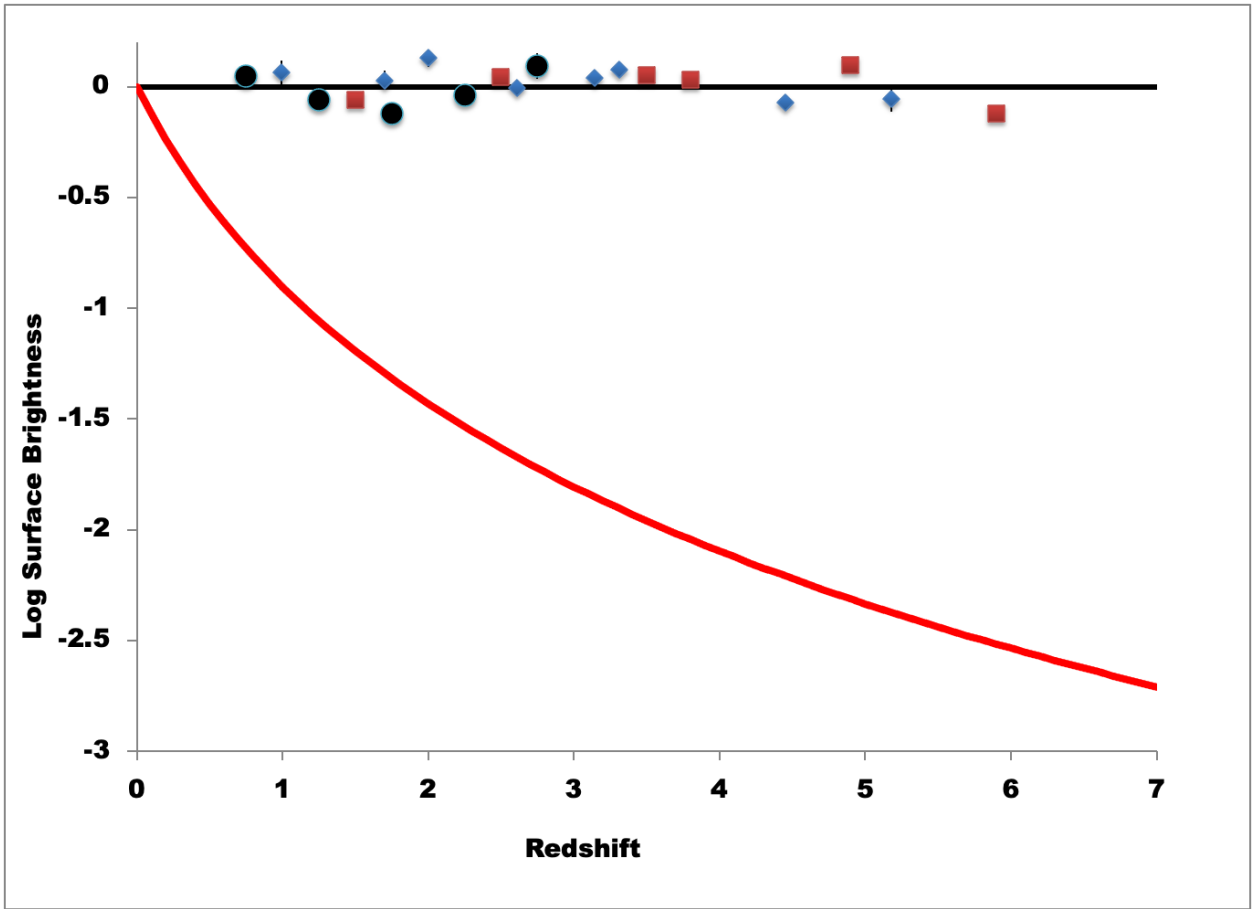

Figure 14. *Luminosity-binned disk and elliptical galaxy data plotted together, with the x-axis being the log of the observed radius to that at low-z, assuming no expansion. The observed data are an excellent fit to the non-expansion prediction of no change in radius for given luminosity, which is the same as no change in SB. Elliptical galaxies are from van de Wel et al, 2014). Large dots are galaxies with mean log L=10.75 while small dots are galaxies with mean log M =11, where L is V-band luminosity and M is stellar mass, both in solar units. Red squares are UV-bright disk galaxies M ~-18 from Shibuya et al, 2015 and the GALEX point at z=0.027 from Lerner, Scarpa and Falomo,2014.*

As can be seen in Figure 14 the whole data set is an excellent fit to the non-expanding hypothesis. The χ^2 for the combined sample is 21 for 20 degrees of freedom. The mean difference in log r of all samples is 0.0041. The best-fit slope on log(1+z) is 0.016+-0.033, again indistinguishable from the predicted zero slope. We also showed how other authors' data is compatible with this conclusion (Lerner *et al*, 2014).

As noted above, for these comparisons we adopt the simple hypothesis that the relationship $d= cz/H_0$, well-assessed in the local Universe, holds for all *z*. It should be noted that this is not the Einstein-De Sitter static Universe often used in literature.

The choice of a linear relation is motivated in part by the fact that the flux-luminosity relation derived from this assumption is remarkably similar numerically to the one found in the

concordance cosmology, the distance modulus being virtually the same in both cosmologies for all relevant redshifts. As shown in Lerner, 2014, up to redshift 7, the apparent magnitude predicted by the simple linear Hubble relation in a Static Euclidean Universe (SEU) is within 0.3 magnitude of the concordance cosmology prediction with Ω_M= 0.26 and Ω_Λ= 0.74. Within the range of the supernova data the maximum difference is only 0.18 magnitudes.

In the past year, Lee (2020), Kang (2020), and other researchers have pointed out that there is a strong correlation between SN1a absolute magnitude and the age of the galaxies, a correlation that leads to a dimming of SN1a by 0.25 mag at z=1. Taking this effect into account to correct the SN1a luminosity distances leads to the *best empirical fit to the data being within 0.07 mag of the linear Hubble relation at all redshifts up to z=1, while the distance to the concordance prediction increases to 0.25 magnitudes.* The linear relation is now a better fit than the concordance curve.

Since the luminosity is almost exactly the same for a given galaxy with the expanding and non-expanding hypotheses, any analysis of *observed* SB, even assuming expansion, should agree with our analysis. Indeed, just recently Whitney et al (2020) *reported absolute constancy of observed SB with redshift out to z =6 with a sample of over 1500 galaxies*. These authors also arrive at the same conclusion as we do that size evolution can't explain the drastic change in SB that appears to occur if expansion is hypothesized. However, accepting expansion, they conclude that there must be a low-SB, high-z population that is missed by present observations.

But this explanation is also ruled out by the data. Since the sample selected in Lerner, Falomo, and Scarpa consist of the most UV-luminous disk galaxies, their closely Gaussian distribution of SB can be detected at all observed z as can be seen in figure 6 of that paper.

The surface brightness/size data clearly conform to the predictions of a non-expanding universe and contradict those of an expanding universe. This necessarily implies that some presently-unknown process causes light to lose energy as it travels long distances. This would be *the single "new physics" hypothesis required by the rejection of the BBH*, as compared with the four new-physics hypotheses (inflation, dark matter, dark energy, proton decay) required for retaining BBH. It should be noted that the linear distance-redshift relationship hypothesized here is different from the exponential relationship hypothesized by many "tired-light" theories.

In addition, such an hypothesized process of energy loss can be studied experimentally on scales well within reach of space craft. For example, a set of spacecraft similar to the proposed LISA array, spaced at 5 million km, could detect with existing technology a shift in frequency at a level of about one part in 10^{18} (Nicholson, *et al*, 2018), which could measure a redshift -distance relation to an accuracy of about 2%. The detection of such a frequency shift, of the order of the Hubble relation, would of course rule out an expanding-universe model, as there is abundant evidence that the Solar System is not expanding.

Even in the absence of such an experiment, the surface brightness and size data is incompatible with the Big Bang expanding universe hypothesis and completely in accord with the non-expanding prediction. They are thus also in accord with the absence of a dense, hot epoch, an absence hypothesized by the GOLE theory.

7. SNIa light curve widths

Another prediction of an expanding universe is the apparent slowing of time in observations of high-z objects, an effect not predicted to occur with a non-expanding universe expected on the basis of GOLE. Goldhaber (2001) and others have claimed that the width of SN1a light curves show exactly the 1+z dependency expected with expansion. However, as Crawford (2017), has pointed out, the width data used were not the actual measured widths, but rather widths corrected with respect to templates of standard widths for each rest wavelength range. These templates contain a strong correlation of wavelength with width. This in turn is derived from calculations that *assume* the validity of the 1+z increase in width. So the results of Goldhaber et al are based on a circular argument: assuming a 1+z correlation for width leads to a wavelength-width dependency that then gives back the assumed 1+z correlation. The wavelength and redshift dependencies are related because of the fixed filters used for observations and thus the strong negative correlation of rest wavelength and redshift.

To actually test the 1+z assumption against observations, Crawford instead used the raw data from the PanSTARSS database to measure the widths of the light curves from supernova, as observed at Earth through various filters. When this actual data for widths are plotted against 1+z there is no correlation at all measured (Crawford 2017).

Crawford's analysis assumes that there is no intrinsic dependence of width on wavelength. Duplicating this analysis, we here re-analyze Crawford's width data, using only the best-fitted light curves, with width error of 5% or less. These are 1090 width measurements out of a total of 3209. In Fig 15(a) we show log w plotted against log (1+z). Confirming Crawford's result, there is no correlation at all.

However, this does not take into account any *actual* correlation of width with rest wavelength. We now take this correlation into account, without any cosmological assumptions, by correlating the width simultaneously with 1+z and rest wavelength λ to minimize the total χ^2 of log w as a linear function of log (1 +z) and log λ.

This minimization results in a correlation of log w = 0.42+- 0.04 log λ. In Fig. 15 (b) we plot the width index I = log w -0.42 log λ against log (1+z) with the same vertical scale as fig 15 (a). The better correlation is obvious and corresponds to a decrease of 14% in χ^2 . The correlation of the width index on log (1+z) is here log I= 0.25+-0.1 log(1+z) and the correlation coefficient r =0.08. This is significant, although barely so, at the 99% confidence level. By contrast, using this model-free analysis, the slope of 1 predicted by an expanding-universe hypothesis is ruled out at a 7.5 σ level.

If we instead *assume* that the expanding universe hypothesis is true, and force the dependency of log I = log(1+z), then the data requires that log w = 1.63 Log λ, an almost 4 times larger slope than in the minimum variance analysis. In fig 15(c) we then plot log I_c = log w -1.63 log λ against log (1+z), again with the same vertical scale. The greatly worse correlation is again obvious, with χ^2 increasing by 89% over the value of minimum-variance analysis in fig 15 (b). Even if we ignore Crawford's width error estimates and simply measure the variance of the width values, then σ^2 for the expanding universe assumption is 79% larger than for the minimum-variance case. Once again,

even taking into account the observed variation of width with wavelength, the expansion hypothesis is completely incompatible with the observations.

The marginally significant correlation of log I with Log (1+z) is not predicted by a non-expanding model. But the significance of this relatively small trend, amounting to a change in width of 19+-8% at z=1, *entirely disappears when the data are corrected for the correlation found by Kang (2020) of SN width with age.* From the data in Fig. 11 of Kang (2020) there is a decrease in the x1 factor with increasing age that corresponds to an increase in stretch by z=1 of 10+-3%. Correcting for this increase reduces the change in width up to z =1 to 8+-8 % and the slope of log I on log(1+z) now becomes 0.11+-0.1, which is not significant. Kang et al's analysis of the correlation is entirely based on SN at low z<0.08, so are not affected by assumptions about width dependence on z or wavelength.

Our new analysis, taking into account both the observed variation of width with wavelength and the observed decrease in width with age, confirms Crawford's conclusions and shows that for the SN1a width data, the predictions of an expanding universe are contradicted and the data is entirely compatible with the predictions of a non-expanding universe.

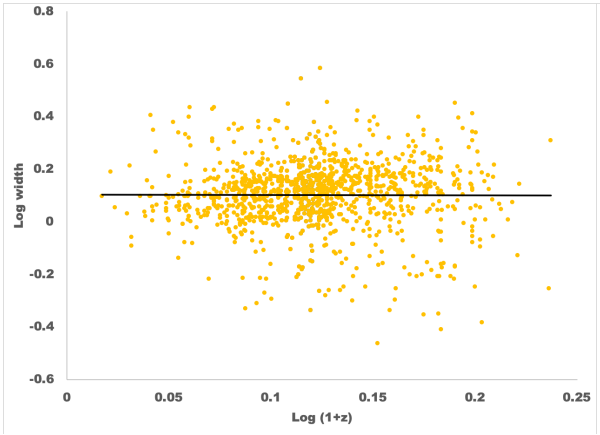

a

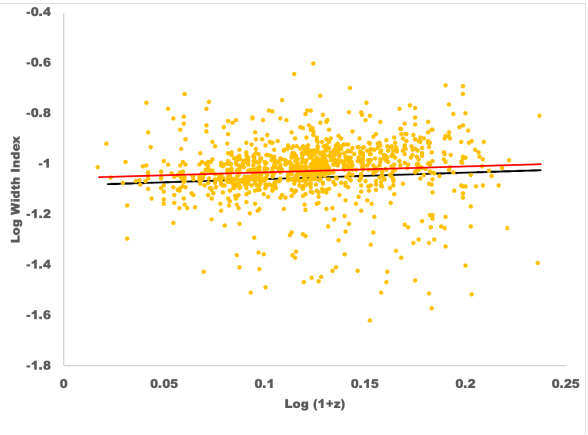

b

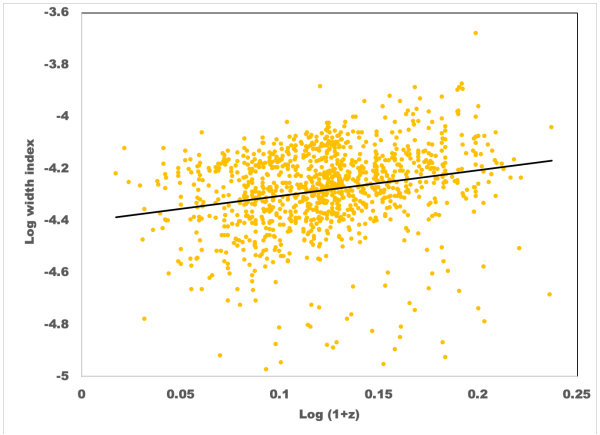

c

Fig. 15 a) Log w (width) vs log (1+z) for uncorrected width measurements of SN1a in the PanSTARSS survey (data from Crawford). Fit (black line) is statistically indistinguishable from horizontal with no correlation. b) log I (width index) accounting for 0.42 slope of w on l shows 0.25 +-0.1 slope of I on log (1+z) with black line minimum χ^2 fit and red line fit assuming equal errors. In neither fit is expansion assumed. Note the reduced variance compared with (a). c) log I_c with slope of 1.63 of w on l, assuming expansion and thus fixing a linear relationship of I_c and 1+z. Note the greatly increased variance as compared with (b).

8. The Cosmic Microwave Background Radiation

A fourth and final major difference in implications between BBH and GOLE concerns the cosmic microwave background radiation (CMB). For the BBH, the CMB is the extremely redshifted radiation from the initial hot, dense Big Bang epoch. However, the CMB, which is highly thermalized and highly isotropic, does not constitute direct evidence of such an epoch. Rather it is direct evidence that, at some point in cosmic history, the universe must have had a high optical depth for the wavelength band covered by the CMB.

Observations show that the CMB spectrum follows a black body spectrum to within about 5 x 10^{-5} in the frequency range from 40-200GHz (wavelength band 1.5-7.5 mm) and to within 5 x10^{-4} in a broader range from 20-400GHz (0.75-15 mm). The CMB is also isotropic to with a few parts in 10^5. Since the deviation of a spectrum from a blackbody depends on optical depth

$$12)\ F(\nu) = 1-e^{-\tau(\nu)}$$

, where F(ν) is the ratio of observed flux at a given frequency to blackbody flux and τ (ν) is the optical depth at that frequency, then the CMB observations directly imply an optical depth of ln (2 x 10^4) = 10 for the narrower frequency band and ln (2x10^3) = 7.6 for the broader band. The CMB observations thus demonstrate that the average photon in these bands has suffered 7.6-10 large angle scatterings or, equivalently, the same number of absorptions and re-emissions, from initial emission to observation.

The question then is: what conditions produced such a high optical depth in these frequency bands? For the BBH, the conditions were a hot dense plasma at a temperature of about 10^4 K, producing a black body spectrum that was then redshifted a few thousand-fold to the present bands. But for three decades, there has been an alternative explanation for the CMB. That is that the energy for the CMB derives from the thermonuclear reactions in stars that produced the observed abundance of He, and that the radiation is thermalized and isotropized by the intergalactic medium, which has a high optical depth in the present frequency bands of the CMB (Lerner,1992).

Despite the widespread popularity of the BBH explanation of the CMB, the test of its validity remains its ability to correctly predict observations. In the past five years, and especially in the past two years, multiple predictions of the BBH theory of the CMB have been contradicted by independent data sets. The failure of the predictions of the theory for H_0 in particular have led to a growing awareness of a crisis in cosmology.

8.1 Quantitative Predictions of BBH Theory of CMB vs Observations

In assessing any theory, it is crucial to compare predictions with *subsequent* observations. In the first 30 years after the discovery of the CMB, the quantitative predictions of the BBH theory of the CMB were consistently contradicted by subsequent observations, which was then followed by the addition of ad-hoc hypotheses to the theory to fit already-observed data. The BBH hypothesis in its original form did not predict a smooth isotropic CMB because there was no mechanism allowing distant parts of the sky to reach equilibrium with each other during the Big Bang expansion. This required the introduction of the inflation hypothesis in 1980, an entirely ad-hoc hypothesis introducing a new inflation field that is not otherwise observed. Second, the original predictions for the amplitude of small fluctuations in the CMB, about 10^{-4} to 10^{-3} [6], turned out to be far too large compared with observations of fluctuations of at most 10^{-5}. This observation required the introduction of the hypothesis of non-baryonic or dark matter (DM) in order to produce large-scale structure.

However, the inflation hypothesis predicted a flat universe with $\Omega_{tot} = 1$ and thus predicted a total dark matter density that was also close to $\Omega_m = 1$. By the mid-1990's the CDM model also encountered gross contradictions with observations. In particular, as measurements of the Hubble relation improved, this model predicted an age for the universe of about 8 Gy (Krisciunas, 1993). This was far too short, as evidence from both individual stars and galaxies indicated. As well, the predicted deviation from linearity of the Hubble relation for supernovae was not observed. This led to the ad-hoc introduction of yet a third hypothesis, dark energy, (also termed the cosmological constant) symbolized by Λ, thus producing the current ΛCDM model (Primack, 1995).

This complex model, despite its many ad-hoc additions, retains testable predictions. Inflation by itself predicts that the fluctuations in the CMB should be isotropic and Gaussian—a random pattern—and that the geometry of the universe should be flat (Schwarz , *et al*, 2016). When further complicated by additional hypotheses, the ΛCDM also predicts the exact amplitude of the fluctuations' spatial spectrum with the adjustment of at least 8 free parameters: the mass density of baryonic matter, dark matter, neutrinos and dark energy, the optical depth at the time of reionization, the "bias factor" (relating the clumping of dark matter and baryonic matter), the

number of neutrino species and the Hubble constant. This list, however, **assumes** the flatness of space. If that prediction is also to be tested, there are (at least) 9 free parameters to the model.

In the late 1990's this new model did begin to claim accord with subsequent observations. In 1996, analysis of COBE observations indicated that the anisotropies in the CMB were Gaussian at all scales, as predicted by inflation (Primack, 1995). By 2003, based on early results from WMAP, published fits of the power spectrum of CMB anisotropies claimed close agreement with the H_0 and total matter density obtained by independent fits to the SN1a luminosity-distance correlations (Hinshaw, et al, 2003). In 2006 additional data analysis (Sanchez, et al 2006) showed a fit to the inflation prediction of a flat universe and good correspondence to the power spectrum all the way to the largest modes, although the largest, quadrupole mode seemed surprisingly small.

Thus by 2006, it appeared that the ΛCDM variant of BBH, with its 8 free parameters, had made at least five independent quantitative predictions that were in accord with subsequent observations. However, there were already clouds on the horizon. As early as 2004, a number of analyses (Schwarz et al, 2004) started to point out significant deviations in the WMAP data from Gaussianity. Further releases of WMAP data, and especially the release of multi-year Planck data after 2013, confirmed and greatly strengthened these analyses so that by 2016 published analyses (Schwarz et al, 2016) showed that the prediction of Gaussianity was clearly contradicted.

These contradictions occur on the largest scales observable—in this case the angular scales larger than a few degrees (ℓ<30). All of the CMB contradictions have been discussed widely in the literature, by many authors, with Schwarz et al, 2016 providing a convenient summary. Isotropy is strongly contradicted because the octopole mode is strongly planar, and because the quadrupole and octopole planes are aligned with each other and aligned with the CMB dipole, theoretically produced by the Solar Systems motion through the CMB (Fig.16). In addition, the total amplitude of fluctuations varies according to the hemisphere of the sky observed and the odd multipoles have different power than the even multipoles, particularly in the range 20<ℓ<30 (Fig. 17). A recent analysis (Yeung & Chuy, 2022) shows that the calculated predictions of cosmological parameters from the Planck data shows strong anisotropy as well. The theory predicts strong correlation of the CMB at large angles, but the correlations at angle>70 degrees are far smaller than predicted (Fig. 18). Each of these contradictions, which are independent of each other, have a probability to occur by chance of less than 0.5% (if inflation were a valid hypothesis) and therefore have negligible probability, less than one in 10^7, taken together.

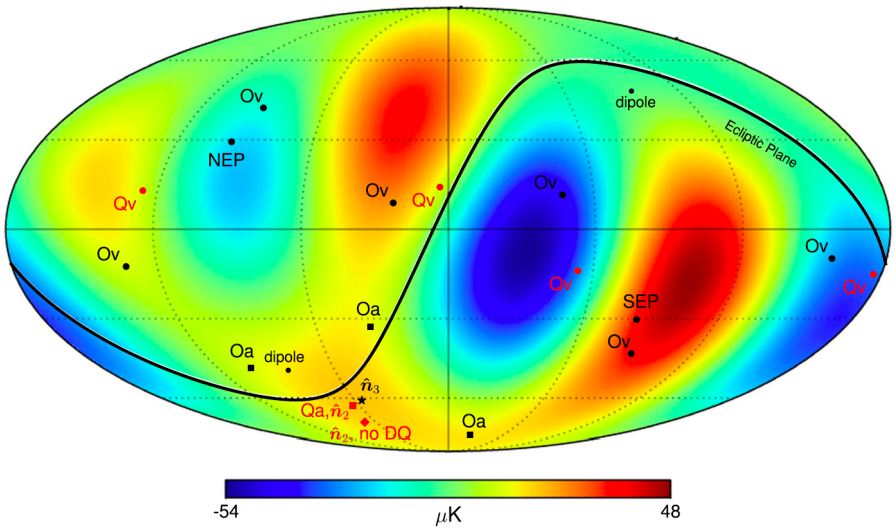

Figure 16. The quadrupole and octopole pattern from Planck (Copi et al, 2015). The obvious planar pattern completely contradicts the predicted random pattern. The three octopole axes (Oa), the quadrupole axis (Qa) and the dipole lie far too near each other, sharply contradicting the theoretical prediction that they be randomly scattered on the sky.

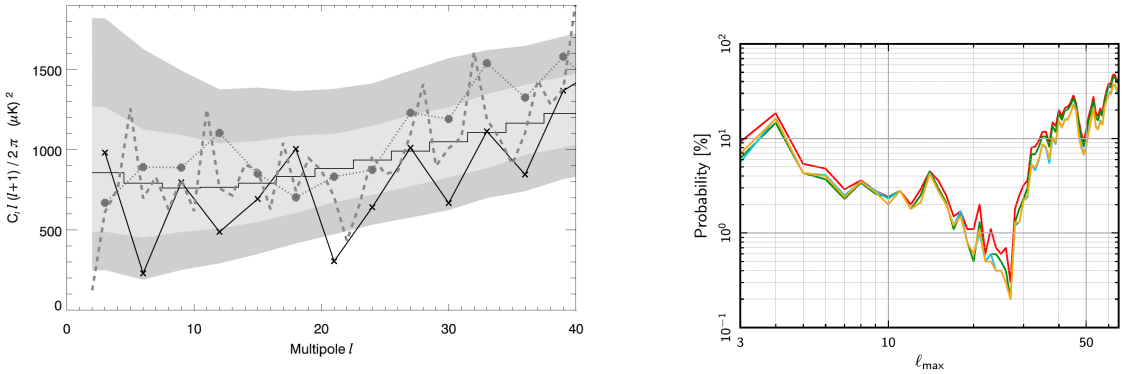

Fig. 17. (a) The CMB fluctuation amplitude is plotted against mode number for the northern hemisphere (solid line), the southern (dotted line) and the whole sky (dashed line) (Schwarz et al, 2016). The theoretical fit's 1σ and 2σ limits are indicated by the light and dark grey shading. The southern hemisphere power exceeds the northern for 11 of 13 modes in this entire range and in all points 20< ℓ<40. For ℓ=6 and ℓ=21, the southern power exceeds triple the northern and is more than double for ℓ=12. (b) The probability of equal power in odd and even modes for $\ell > \ell_{max}$ (Schwarz et al, 2016). The deviation from isotropy is maximized in the same angular range as for the hemisphere asymmetry and the direction of maximal asymmetry is close for the two types.

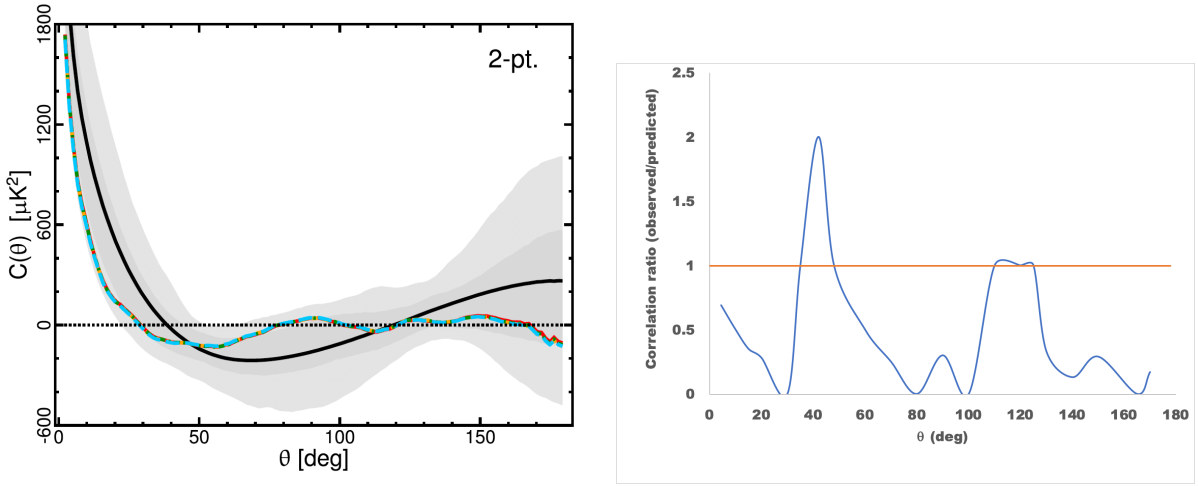

a *b*

Fig. 18 (a) Comparison of observed two-point correlations of the CMB vs angular separation (Schwarz et al, 2016). The black line is the prediction, the grey area the 2 σ limits and the blue line the Planck observations. Despite the observations being at any given point within the 2 σ limits, the prediction is a highly improbable fit to the observations. This is made more obvious when the same data is replotted (b) here as a ratio of the absolute value of the observed correlation to the predicted one. Except for the small regions around the predicted zero crossings at 40 and 115 degrees, the observed correlations are all much smaller than the predictions, while one would expect about half to be larger.

By the same time, Planck data made clear that for the power spectrum, the best fit curve for ℓ>30 was a poor fit for ℓ<30. In particular, as can be seen if Figure 19, the strong dip in amplitude in the range 15<ℓ<30 is entirely missed in the predicted curve. This is the same range as for the greatest parity and hemispheric asymmetry. So even with 9 free parameters, the entire data set can't be accurately fit. Thus by 2016, published analyses unequivocally demonstrated that two basic quantitative predictions of the BBH theory of the CMB were contradicted by better data.

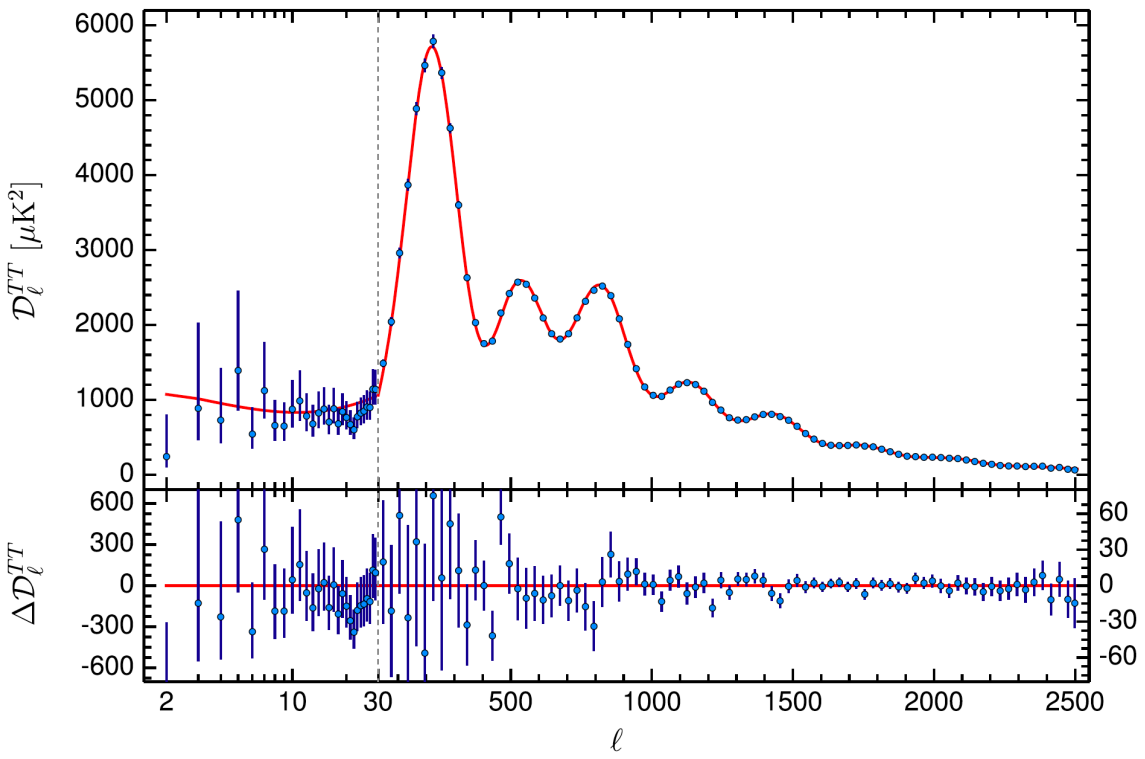

Fig.19 Angular band power (top) and residual angular band power (bottom) of the cosmic microwave temperature anisotropies (Schwarz et al, 2016), based on Planck 2015 data. Note the change of scale at ℓ=30. The deviation of the data is clear in the range 15<ℓ<30.

In the past two years, the three remaining quantitative predictions have been contradicted by data. Handley (2019), Park&Ratra (2019) and DiValentino *et al*, (2020) have shown that when the curvature parameter is allowed to vary, the best fit to the power spectrum is not a flat universe, contradicting another basic prediction of inflation. It is important to emphasize. that without inflation, the BBH does not even predict an approximately isotropic CMB, so is grossly contradicted by the observations of fluctuations at the level of 10^{-5}.

The CMB considered by itself thus provides extremely serious contradictions to BBH predictions. There are as well additional serious contradictions when the BBH fit to the CMB power spectrum is used to make predictions about other data sets. In the past two years, much attention was given to the fact that the value of the Hubble constant predicted by the fit to the CMB spectrum is different from the value actually measured by comparing the distance to supernovae with their redshifts, with the difference now reaching 4-6 σ (Riess, 2020). While this has been described as a difference between two measurements, it is in fact another failure of a theoretical prediction, based on fitting the CMB spectrum with the help of Big Bang theory. The only direct measurement was based on the supernovae data, which compare two observable quantities, the apparent brightness of the supernovae and the redshift of their spectrums.

It is important to note that the work over the past two years by Kang *et al* (2020) and others showing the correlation of stellar population age with SN1a luminosity has demonstrated that when

this correlation is taken into account, the SN1a data are best fit (assuming the BBH) with $\Lambda = 0$. Since the CMB power spectrum is fit with $\Lambda = 0.7$, this demonstrated yet other contradiction in the BBH predictions.

Another extremely significant contradiction is in the prediction, based on CMB fitting and the ΛCDM model, for the density of dark matter. There is convincing evidence from multiple data sets that non-baryonic matter does not exist at all **(**Adhikari, G., et al,2018; Aprile, E. et al. (XENON Collaboration),2018; Kroupa, P. Pawlowski, & M. Milgrom, M,2012; Müller *et al*.,2018)**.** But the ΛCDM model, combined with the CMB fitting, also predicts the total amount of gravitating matter. In the flat universe fit, this total is close to $\Omega_m = 0.3$. If flatness is not assumed, the best fit predicts even more matter, around $\Omega_m = 0.5$ (Schwarz et al, 2016). But this prediction for total matter density is strongly contradicted by measurements that relate galaxy cluster distribution to observed velocities of bulk flows of galaxies. These studies (Karachentsev, 2012) show that even on large scales $\Omega_m < 0.1$, which is 10 σ from the BBH predictions.

Thus, taking together the large-scale asymmetries, the poor fit at large angles, the contradictions with flatness predictions, the wrong prediction of matter density and the widely-discussed wrong prediction of the Hubble relation, the BBH predictions of the CMB are amply falsified. At present, no quantitative predictions of the BBH for the CMB are in accord with observations. As DiValentino *et al* summarize: "BAO surveys disagree at more than 3 standard deviations. CMB lensing is in tension at the 95% CL. The R18 constraint on the Hubble constant is in tension with PL18 at more than 5 standard deviations, while cosmic shear data disagree at more than 3 standard deviations. These inconsistencies between disparate observed properties of the Universe introduce a problem for modern cosmology: the flat ΛCDM model, de facto, does not seem any longer to provide a good candidate for concordance cosmology…"(DiValentino, Melchiorri and Silk, 2020) .To this we add only that the "flat ΛCDM model" is the current version of the BBH.

This is not the viewpoint of a small fraction of researchers in the field. A comprehensive survey of the "anomalies" between concordance cosmology and observations by some 200 authors (Abdalla *et al*, 2022) listed at least 22 such contradictions.

8.2 The non-expanding (GOLE) theory of the CMB

There is an alternative explanation of the CMB that does not require a Big Bang. As has been noted repeatedly in the past and is pointed out again in section 4.2, the energy needed to account for the microwave background is comparable to the energy that would have been released by the production by ordinary stars of the known amount of helium, as predicted by GOLE.

Calculations in section 4.2 and earlier papers predicted a thermonuclear energy release of 4 Mev/H. Given this value, the known CMB energy density of $0.26 eV/cm^3$ would be produced from a total H density of $6.6 \times 10^{-8}/cm^3$. By comparison, the baryonic density in the current BB model is $2.5 \times 10^{-7}/cm^3$ while actual observations of hydrogen density on large scales are around $1.2 \times 10^{-7}/cm^3$. Using this latter observational value predicts an energy release that is greater than that needed to produce the observed 2.73 K background radiation temperature, if it is thermalized to equilibrium.

The isotropy and black-body spectrum of the CMB are inevitable if the *present-day* intergalactic medium has sufficient optical depth in the microwave band. The present author proposed (Lerner, 1988) along with others (Peter and Peratt, 1990) that the CMB is a radio fog permeating the present-day universe, not some ghost of a long-ago Big Bang. As Planck demonstrated in deriving the blackbody spectrum, *any* body with high optical depth must radiate with a blackbody spectrum.

There is a clear-cut test for the hypotheses that there is a significant optical depth in the present-day universe. If the universe scatters or absorbs microwave and radio radiation, but is transparent in the shorter-wavelength infrared bands, then more distant objects will appear dimmer in radio bands then in IR. Observational evidence (Lerner, 1990, 1993) of this absorption effect comparing 60μ−100 μ IR with 1.4GhZ radio showed that radio emission by galaxies dropped **by a factor of 10** as distance increased to 300 Mpc. This work showed that for nearby galaxies with redshift $z<0.07$, radio emission for a given IR luminosity falls as $z^{-0.32}$. (Fig. 20) A zero correlation with z, as would be expected in an IGM fully transparent to radio radiation, was excluded at a 5 σ level in (Lerner, 1990) and at an 8 σ level in (Lerner, 1993).

This distance of 300 Mpc corresponds to a look-back time of only 900 My, too short a time for any evolutionary process to create such a dramatic change. An evolutionary process accounting for this change in brightness with distance would have to accelerate unphysically as it approached the present, with galaxies doubling in brightness in the last 10 million years alone.

This strong decrease in radio emission with z was overlooked by many other researchers, because the widespread measure of the radio-IR relationship is q, the log ratio of IR to radio emission. This measure assumes a linear relationship between the two luminosities. However, it has long been clear that the actual relationship is non-linear. As Devereux and Eales (1989) first found and later work (Lerner, 1990) confirmed, the $L_r \sim L_{IR}^{1.29}$. Since mean L_{IR} is steeply correlated with z, therefore at higher z, more luminous galaxies are observed, with higher radio-IR ratios (lower q). This effect obscures the fall with z in radio luminosity for the same IR luminosity. Simply analyzing the data among the three variables simultaneously yields the nonlinear radio-IR relationship and the steep decrease in radio luminosity with z.

This evidence of radio luminosity decrease is here further extended to 600 Mpc with new data at 150 MHz. Using LOFAR and IRAS data, Wang et al (2019) found that

13) $L_{150} \sim L_{IR}^{1.37+-0.045}$

The re-analysis here of Wang et al's data presented here uses the 412 galaxies identified as star-forming or starburst, excluding broadline galaxies and AGNs. This shows a dependency of $L_{150} \sim L_{IR}^{1.29+-0.048}$, in statistical agreement with Wang's and with the 1.29 slope found previously by Lerner and Devereux and Eales for 1.4GHz (fig. 21). A linear slope is ruled out at a 6 σ level. The same analysis shows that the radio luminosity for a given L_{IR} declines as $z^{-0.42+-0.087}$, (Fig.20 b) again in good agreement with the exponent of -0.41+-0.06 in (Lerner, 1990)and -0.32+-0.04 in (Lerner, 1993). The zero slope expected with a transparent IGM is ruled out again at a 4.8 σ level.

This is an example of an assumption, made in support of the BBH, of a relationship among multiple variables that is not supported by data. A second one is the assumption of a flat universe in the

analysis of the CMB. Eliminating these false assumptions, and using instead the correlations derived from the actual data, makes clear the contradictions between the BBH predictions and the data.

At higher redshifts, present data makes measurements of radio luminosity more model-dependent, since they depend on K corrections at both IR and radio wavelengths, which are uncertain, and any changes in the radio-IR relationship could be attributed to evolution. However, spectra of ULIRGS at high z (fig. 22) show a reduced ratio of FIR to NIR radiation(Sajina, et al, 2012) as would be expected if absorption or scattering occurs at wavelengths longer than about 200 μ. This effect also could be attributed to evolution, but is entirely consistent with the predictions of an opacity model.

The data presented in fig. 20, while limited in z, can be used to estimate a range of optical depths for the IGM. It is important to note that the data itself, with no extrapolation, already shows an absorption of a factor of ten, and thus an optical depth $\tau = 2.3$, 30% of that needed to account for the CMB spectrum in the frequency range up to about 20GHz. We also note that the fit to a power law dependency on distance is consistent with a fractal distribution of scatterers or absorbing objects with fractal dimension of 2. Such a density distribution would reflect the observed fractal distribution of galaxies (Telesa et al, 2021) .Thus, if density $n = k/D$, then the optical depth $\tau = k \ln D/\text{Mpc} - \ln D_0/\text{Mpc}$, where D_0 is the distance where the fractal rise in density plateaus. The observed luminosity after absorption or scattering then is proportional to $e^{-\tau}$ or D^{-k}, thus producing the observed power law.

The absorption can be extrapolated to large distance if we hypothesize at what distance, D_H, the fractal distribution of density levels out into a homogenous distribution. We take the minimum D_H to be just the maximum distance already observed in the data—600 Mpc. The maximum D_H is equal to the 1.5 Gpc radius of the largest inhomogeneities observed at present(Shirokov et al, 2016). We take D_0 to be 1 Mpc as a maximum, since the data shown in fig. 20a shows no sign of a plateau at larger D.

We are assuming a non-expanding, non-BBH universe as described by section 6, with $D= cz/H_0$. With this assumption and the hypothesized range for D_H we then can calculate that an optical τ = 7.6 will result for absorption up to a z=2.2+-1.0 and τ = 10 will result for a z = 4.3+-2. It is thus clear that extrapolating the observed radio absorption produces the right order of magnitude of τ needed to produce the observed CMB blackbody spectrum and isotropy.

This data is limited to frequencies well below those in the frequency range 20-400GHz where the CMB is closest to a blackbody. Future work will look at higher frequency data. However, there is no evidence that the optical depth of the IGM decreases sharply with increasing frequency above 1 GHz. If this were the case, localized sources at substantial z would show a kink in the spectrum, with the slope α of I_ν on ν decreasing in the region of ν>1 GHz. But this is not observed. For example, a sample of sources selected at 15.7 GHz show a median α of -0.6(Whitman et al, 2015), essentially the same α as for the MW and other galaxies measured in the range ν<1 GHz.

8.3 Mechanisms for absorption or scattering

There are at least two phenomena that could account for the absorption of microwave and RF radiation. One is that radiation in these wavelengths could be absorbed and reemitted by electrons trapped in dense plasma filaments emitted from a range of astrophysical jets extending from stellar Herbig-Haro objects to quasars (Lerner, 1993). In addition, other researchers have pointed out that spinning dust particles can also absorb and re-emit microwaves (Draine &Lazariuan, 1998). We do not consider this hypothesis further here.

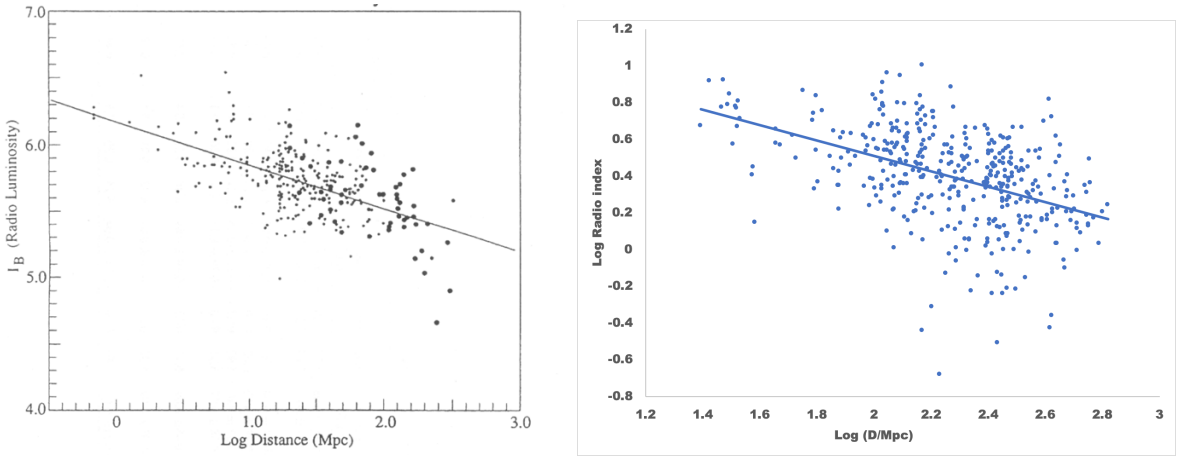

a b

Figure 20. The logarithm of radio luminosity of galaxies with the same IR luminosity plotted against the log of the distance. The correlation can only be explained by a strong absorption in the IGM. (a) (From Lerner, 1993). 1.4 GHz luminosity. The solid line is a fit to the data of $I_B \sim z^{-0.32}$. *(b) New analysis for 150 MHz luminosity based on data from Wang et al, 2019. Log radio index* $I_r = \text{Log } L_{150} - 1.29(\text{Log } L_{IR}) + C$, *where C is an arbitrary constant. The solid line is a fit* $I_r \sim z^{-0.42}$. *The data in (b) extends outward in distance a factor of 2 further than those in (a), to 600 Mpc.*

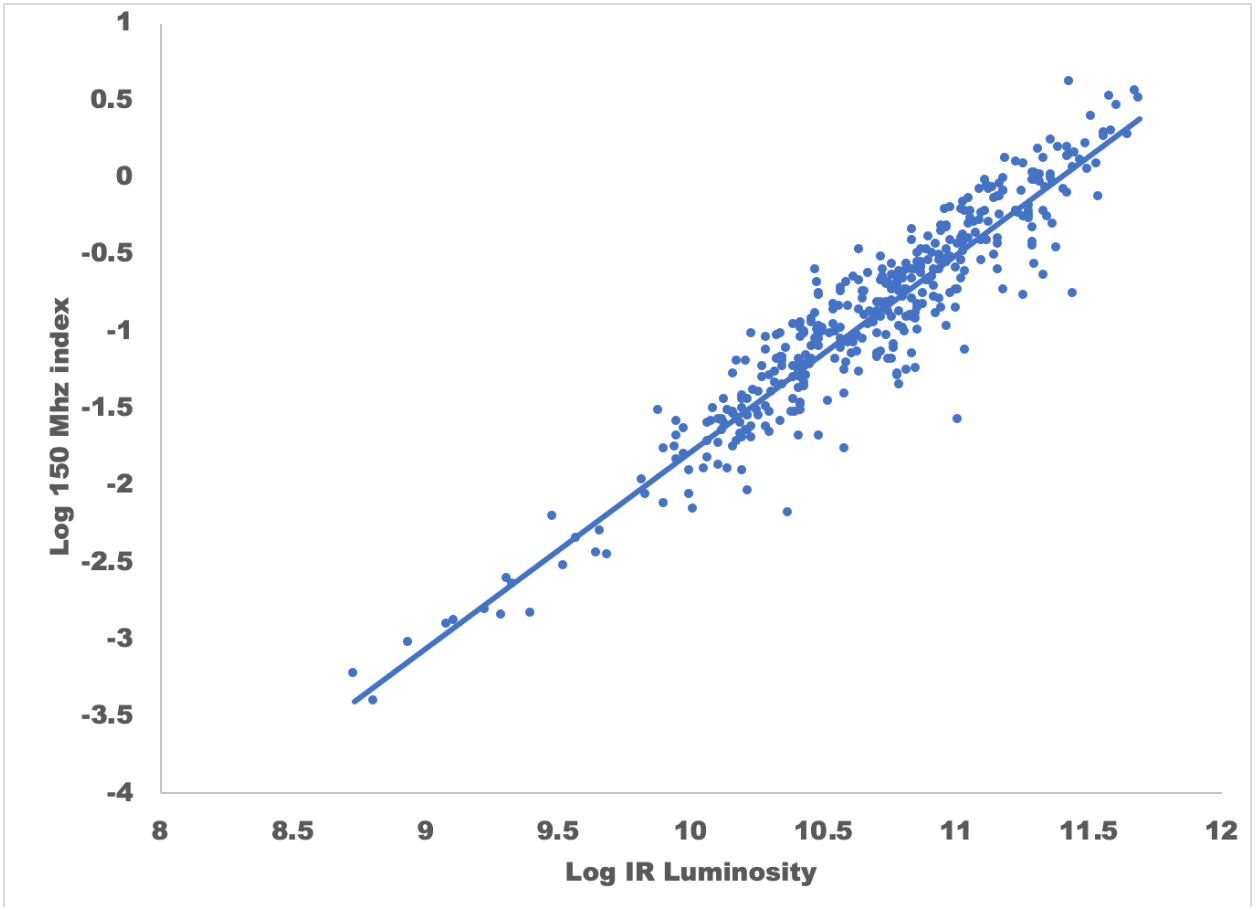

Fig. 21 Same data as Fig.20 b, but plotted to show dependency of Log radio index I_r'= Log L_{150}+0.42(Log z) + C'. The solid line shows the minimum variance slope of 1.29, showing clearly the non-linear relation of radio and IR luminosity, when the decrease with z is independently accounted for.

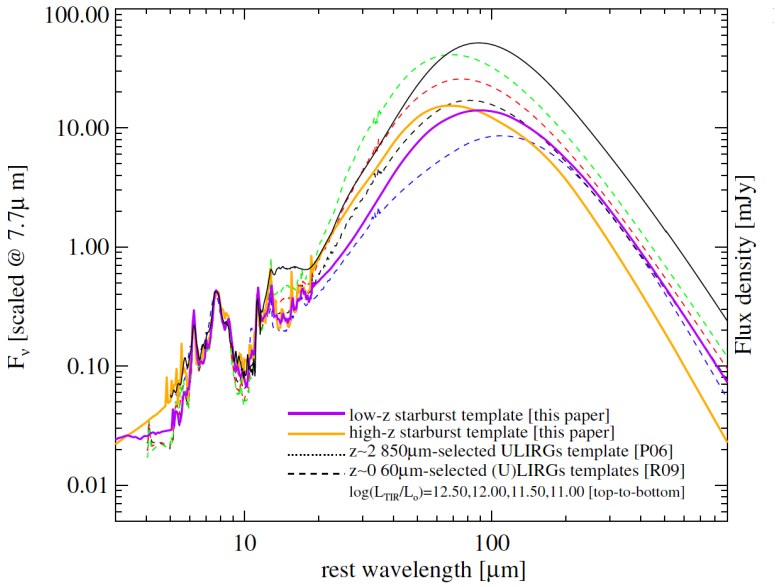

Fig. 22. The average spectra of high-z starburst galaxies (orange curve) shows a decrease relative to the low-z spectra (purple curves) for wavelengths >100μm, consistent with the existence of an absorbing/scattering IGM. (From Sanjina, et al, 2012)).

The discovery (Leitch et al, 1997) of anomalous microwave emission (AME) from clouds in the Milky Way confirms that there exist processes that efficiently emit, and therefore can absorb and scatter, radiation in the CMB wavebands. It is important to note that a blackbody spectrum results from *any* collection of absorbers that are sufficiently opaque. Also, scattering at large angle, where the emission angle is uncorrelated with the absorption angle, does not result in blurring of distant objects, as small-angle scattering does.

Recently, evidence has been published of the existence of plasma filaments that are compatible with the filaments were predicted in Lerner, 1992, 1993 to be capable of producing the thermalization of the CMB. In these papers, the present author demonstrated analytically that plasma filaments would form from the beams emitted by QSO's and AGN. For clarity, we here summarize the much more detailed derivations in those papers. Gaussian units are used.

We assume that in the accelerating region of a QSO or AGN ion beam that ions and electrons travel along field lines, that magnetic field energy is approximately equal to ion kinetic energy and that only current carriers are present in the beam (as background particles would be rapidly expelled). We also assume for simplicity a pure H plasma. We then have:

14) $B^2/8\pi = n_i\gamma_p Mc^2$
15) $n_i = B/2\pi er = B^2/8\pi\gamma_p Mc^2$
16) $B= 4\gamma_p Mc^2/er$
17) $I= 2\gamma_p Mc^3/e = 2\gamma_p ec/r_p$

, where B is magnetic field, n is proton particle density, r is beam radius, γ_p is proton relativistic factor, M is proton mass, and r_p is classical proton radius, e^2/Mc^2.

For a beam accelerated to energy $\gamma_p Mc^2$ in length L, synchrotron loss will balance energy gain if

18) $L/c = 24\ Mc/r_p^2B^2\gamma_p$

From eqs (17) and (18) we get:

19) $I^3/L = 12\ (ec)^3\ (r/L)^2/\ r_p^4$
20) $P=2.9x10^{34}\ L^{\ 2/3}\ (\sin\theta)^{4/3}$ erg/s

, where P is beam power and θ is opening angle. Observations(deRutier, 1990) show that $\theta = 2.6\ x10^8\ P^{-0.21}$ so substituting into eq(20),

21) $P = 4.9x10^{35}\ L^{\ 0.52}$ erg/s

For any beam with power larger than that defined by eq (10), the beam will reach a steady state in which it is losing energy to synchrotron radiation as fast as it is gaining in by the accelerating field. These beams are unstable to filamentation, as is demonstrated in Lerner, 1993, since any local increase in magnetic field will cause protons to lose energy to synchrotron energy faster than they are gaining, shrinking their gyroradius, concentrating the currents and increasing magnetic field further. A fractal hierarchy of filaments will thus form with B'^2r' and $B'\gamma_p'$ constants for the whole array, where the primes refer to the filaments within the beam.

For most QSO's and AGN's, emitted power exceeds, in many cases, greatly exceed P defined by Eq (21). For example for L= 0.3 pc, 10^{18} cm, typical of a QSO, P = 1 x10^{45}/erg/s, much smaller than the total energy emission of luminous QSO's (>10^{47} erg/s) while for L= 10^{15} cm, typical of AGN, P = 3 x 10^{43} erg/s, again relatively modest. Thus, most QSO's and AGNs can be expected to produce arrays of filaments.

Once such filamentary beams leave the accelerating region, the electrons and protons will lose energy rapidly through synchrotron radiation. However, such cooling will stop when the *proton* synchrotron frequency is less than the *electron* plasma frequency that is, when the plasma becomes opaque to *proton* synchrotron radiation. In a force free filament, with all particles moving along field lines, the minimum radius of the field lines is defined by the proton gyroradius, so the electrons *moving along the same field lines* radiate at the same frequency as the protons. Since the electrons and protons are counterstreaming, we have

22) $(4\pi n_e e^2/m)^{1/2} = eB\gamma_p'^2\,\gamma'_e/4Mc$

, and since $B'^2/n_e = 8\pi\gamma'_p Mc^2$,

23) $\gamma'^5_p\,\gamma'^2_e = 8M/m$

And, since $\gamma'_e = \gamma'_p$,

24) $\gamma'_p = (8M/m)^{1/7} = 3.94$

As shown in Lerner, 1993, the hierarchical array of filaments will expand, maintaining the constancy of B'^2r' among the filaments, while the value of B'^2r' for the array declines. Eventually the expansion of the array ceases when $B'^2r' = K$, the value for the background plasma. Observations of large-scale magnetic fields indicate K~6 x 10^{12} G^2 cm. For example, for a large galaxy r = 5 x 10^{22} cm and B = 10^{-5} G, so here K= 5 x10^{12} G^2. The number of filaments were calculated in ref 5 (eq 10-11) to also follow a fractal law with fractal dimension D =2. Thus, within an array the number N of filaments of radius r would be proportional to 1/r and the fraction of sky covered by the filaments would be independent of r.

In these filaments, electrons moving along magnetic field lines would be able to absorb and re-emit photons at the *electron* synchrotron frequency only by transiently acquiring and losing momentum *perpendicular* to the field lines. The electrons' energy perpendicular to the lines would be in equilibrium with the background radiation at 2.73 K, but their energy along the field lines would be ~ 2 MeV. Since the electron synchrotron frequency is 1836 times higher than the proton

synchrotron frequency, the highly anisotropic plasma in *these filaments can strongly absorb and emit radiation at frequencies thousands of times above the electron plasma frequency*. This behavior is thus extremely different from that in an isotropic plasma.

The model predicted (Lerner, 1993, eq 3) that a given filament would be highly opaque to frequencies less than the electron synchrotron frequency, which would be correlated with the filament radius:

25) $A = \pi h r_e B^2 R f \ /6kT_p Mc\gamma_e\gamma_p$

, where A is optical depth at the synchrotron frequency, f = abs(νdR/Rdν)=2, for B^2r = K, and T_p is the temperature of electrons perpendicular to the field lines. From eqs (22) and (24)

26) $A = 6.6 \times 10^{-12}$ K

So, the opacity for $\nu < \nu_s$, the synchrotron frequency, is independent of B. For K= 6×10^{12}, A= 40 and thus the filaments are highly opaque. Since

27) $\nu_s = 11$ B MHz

, the frequency range of opacity depends mainly on the range of B in the expanded filament arrays.

The highest B field in the smallest filaments are limited in two ways, as shown in Lerner, 1993. First, the intial $\gamma'_p > 3.94$ and second, the filaments must survive collisional processes during formation and the expansion of the array. In these filaments, the collision distance is far greater than the ion or electron gyro-radius. Because any collision allows particles to move only by one gyro radius across the field lines, but by one collision distance along field lines, conductivity is enormously greater along field lines than across them. This leads to the formation of electrojets, where ions and counter-streaming electrons become segregated in separate streams. Electrojet-formation, driven by the greater rate of collisions that electrons encounter when mixed with ions than when segregated, can't be countered by electrostatic forces between ion and electron streams due to the negligible cross-field conductivity. This conductivity *decreases* with decreasing collision rates, reinforcing the electron-ion segregation.

Electrojet formation reduces collisional energy losses, but detailed calculations in ref 5 show that smallest, densest filaments will dissipate before they have time to expand (see eq 15-31, table 1 in Lerner, 1993). These calculations show that the filament abundance will start to decline slightly for $\nu_s > 150$ GHz and the highest-B filaments will have $\nu_s = 1.4$ THz. These densest filaments will have B = 1.2×10^5G and r =400 cm. Even for these densest filaments, lifetime from collisional losses will be very long, > 1400 Gy.

The maximum filament radius in the filament array will be determined by the synchrotron radiation decay of proton energy to the stable 4 Gev level. As shown in Lerner, 1992, filaments with $\gamma'_p > 7 \times 10^6$ will have B field too small to decay in < 10Gy so will not have electron that cool down to low T_p. The largest filaments will thus have B = 0.07 G and r = 1.3×10^{15} cm or 100 AU (astronomical units). These have $\nu_s = 0.8$ MHz, but another factor will limit the low-frequency

array opacity. Radiation with wavelengths longer than the minimum filament radius of 400 cm will not be scattered by these smallest filaments and thus the opacity of the array is expected to start to decline at $\nu < 75$MHz and Lerner, 1992 predicts a low-frequency cut-off of opacity at 150 MHz.

Comparing these predictions from 30 years ago with current observations, we find that on the high frequency side, the total cosmic background radiation starts to diverge by about 10^{-4} from a blackbody at around 250 GHz and the much hotter, non-blackbody IR background dominates total radiation for $\nu > 800$GHz[32]. This is in good agreement with the predicted transition to transparency occurring between 200 and 1400 GHz.

On the low-frequency side, the background radiation is clearly non-blackbody at 80 MHz (Baiesi,2020;Dowell&Taylor,2018). The data from Wang, 2019 used in section 3 show that there is still high opacity at the observed frequency of 150 MHz, so that transition to transparency occurs between 80 MHz and 150 MHz, in accord with Lerner, 1992. However, the observations are somewhat ambiguous, since at 408 MHz, there is one measurement (Haslam, 1981) of cosmic radiation temperature of 10 +-3.5 K, which is incompatible with opacity at this frequency. But another earlier measurement (Howeel&Shakeshaft, 1967) at the same frequency yielded a radiation temperature of 3.7+-1.2 K, which is compatible with a 2.75 K blackbody.

Do known sources of filament arrays—QSOs, AGNs and possibly Herbig-Haro objects—supply sufficient current and energy to account for the observed IGM opacity in the microwave band? The calculations in Section 3 show that if homogeneity occurs on scales of 1.5 Gpc, then to match observed opacity the arrays would have to have an optical depth of 1 for a depth D of 8×10^{27} cm or 2.6 Gpc. To achieve such an optical depth with filament arrays with maximum radii of r=1.3 $\times 10^{15}$ cm requires a fill-factor of $\pi r/2D = 2.6 \times 10^{-13}$. The magnetic and kinetic energy in the array is of the order of 6×10^{-5} eV/cm^3, only 0.25% of the energy in the CMB and about half that calculated by Lerner[28] for total CR from stars. The total power from QSO's and AGNs has exceeded 10^{41} ergs/s/Mpc ^{3} or 3.7×10^{-33} erg/sec-cm ^{3} for the last 10 Gy[37], which produces an energy density of 7×10^{-4} eV/cm^3. This is a factor of 10 more than in the filament arrays. As pointed out in Lerner, 1992, the amount of matter and energy in the hypothesized fractal array of filaments is not excessive. With a mean ion energy of 4 Gev, even with equipartition of energy between fields and particle, the total ion density due to the arrays is 1.5×10^{-14}/cm^3, so amounts to $<10^{-7}$ of total IGM density.

Recently, observations have provided some direct evidence of the existence of small, energetic filaments. In January, 2021 Wang *et al* (2021) reported observations of a plasma filament that are consistent with those predicted 30 years earlier. They observed five rapid scintillators that were aligned in a straight line across a distance of 2 degrees on the sky. The scintillators, observed at 945 MHz, had a mean deviation from the straight line of 20", indicating that they lay behind a plasma filament that was straight to at least 1 part in 300. By itself, this geometric observation indicated that the internal magnetic forces of the filament were at least 300 times stronger than the background magnetic fields that would tend, over time, to bend the filament. Since the local magnetic field is about 4 μG, this implies that the filament internal magnetic field exceeds 1mG.

Wang *et al* observed variations in the scintillation over the course of a year that showed the filament had a low velocity relative to the Sun close to 10 km/s, which together with other observations led to the conclusion that the filament was about 2-4 pc distant. The radius of the filament at this distance is 0.7-1.5 x 10^{15} cm, just in the upper range of that predicted in Lerner, 1992.

Equally significant, Wang *et al* observed extremely rapid and deep scintillations of the sources behind the filament, as much as doubling or halving of observed flux over a 15-minute period. Interpreting this as being caused by sub-filaments moving across the source, the observed 10km/s velocity implies objects with radii of the order of only 10^9 cm. Since the rapid oscillations are continuous and exceed 50% of signal strength, the number of sub-filaments in the overall filament must be on the order of the ratio of the radii: ~ 10^{15}cm/10^9 cm =10^6, as predicted for such arrays in Lerner, 1992. A significantly smaller number of filaments would lead to intermittent rather than continuous oscillations, while a significantly larger number will smear the scintillations to produce smaller amplitudes than those observed.

For the observing frequency of 945 MHz, eq. (27) combined with $K=B^2r=6x10^{12}$, predicts a filament radius r of 0.8 x10^9 cm, in good agreement with these recent observations. Significantly, other recent observations (Osterloo, *et al*, 2020) have confirmed the existence of the predicted small-radius filaments on the order of 10^9 cm. Observations of scintillation (Koay *et al*, 2019) have extended up to higher frequencies of 15GHz, showing that plasma filaments exist that can affect radiation in the range where the CMB is closest to a blackbody.

Based on the small distance to this filament, Wang *et al* estimate that the optical depth generated by such filaments is ~10^{-3}/pc, which means that they will cover about 0.4 of the sky in the direction perpendicular to the galactic plane, assuming they are confined to within 400 pc of the plane. If we hypothesize such filaments exist in the IGM in numbers proportional to ion density, with the local ion density being about 0.1/cm^3, then the optical depth in the IGM at an ion density of 6 x 10^{-8}/cm^3 would 0.6/ Gpc. This would 30% less than the optical depth estimated above from extrapolating actual observations of RF absorption in the IGM, well within the uncertainties in both estimates.

These observations can be explained by *small-angle* deflections by the plasma filaments, and that is indeed the explanation assumed in the papers reporting the observations. However, they are also entirely consistent with the *large-angle* scattering, actually absorption and re-emission, hypothesized by Lerner, 1992,1993. Further observations and modeling will be required to unequivocally distinguish between these two possibilities. But if the filaments are generating large angle scattering, they would be entirely consistent with both the phenomena responsible for the observed IGM absorption and with the GOLE plasma filament model.

8.4 Conclusions on the CMB

The observation of radio-frequency absorption shows that the production of an isotropic black-body CMB occurs in the present-day universe, although it does not preclude an earlier isotropization by a Big Bang. However, these observations do cast strong doubt on the hypothesis

that the observed CMB fluctuations are created by a Big Bang. The fluctuations are instead dominated by fluctuations in density of the absorbing medium in the IGM. It is significant to note that even the AME already observed in the Milky Way, if typical of other galaxies, would by itself produce fluctuations on the level of those observed. The AME is strongly correlated with H column density[41] at a level of 3 x 10^{-18} Jy cm^2 . With typical IGM column density of the order of 3 x10^{21}/cm^2, AME levels from galactic clouds like those in the MW would be expected to be ~10 kJy, while fluctuations in the CMB are ~4kJy. The actual fluctuations produced by high-opacity objects would of course depend on their nature and distribution, and can't be predicted without further detailed calculations.

However, the evidence presented in this paper shows that only about 8+-4% of RF radiation from >600Mpc distance reaches Earth. Such a strong absorption (or high-angle scattering) has the potential to reduce to low levels any trace of the high degree of inhomogeneity in the IGM, just as inhomogeneities in cloud density become invisible in a heavy fog. However, whether the actual observed inhomogeneities in galaxy distribution can reproduce the observed inhomogeneities in the CMB requires considerable additional research.

So, in contrast to the BBH model of the CMB, the GOLE model, in which the energy for the CMB is supplied by the same fusion reactions that produce the observed helium, and the energy is isotropized and thermalized by the IGM, produces no contradictions with observations, and is confirmed by evidence for the opacity of the IGM at CMB frequencies.

Of course, considerable further work is required to make more detailed comparisons with observations of the fluctuations expected from an isotropizing medium in the present-day universe, and to compare more detailed models of filament arrays with the new observations that will emerge from surveillance with the new phased array instruments. But research resources would be better directed to these questions than to the BBH model of the CMB, which is now contradicted by observations for all quantitative predictions.

9. Discussion

The updated reassessment presented here, comparing the galactic origin of light elements (GOLE) hypothesis with the Big Bang hypothesis, confirms that the GOLE hypothesis is able to correctly predict the abundances of He, Li, D, C, and O, as well as the correlation of Be with O, while BBH only correctly predicts D and is completely contradicted by He and Li data. Specifically, it has been demonstrated in section 4 that ULIRG data confirm the hypothesis that forming galaxies produce He at the high rate predicted by GOLE, and C and O in amounts in accord with GOLE predictions. Updating the GOLE model based on the latest theoretical calculations and observational data confirms that the model predicts the observed abundances of He, D and Li. Taking into account extensive observations showing that most CR are directed downwards towards their star, neutrino data have provided evidence of the amount of CR hypothesized by GOLE. Independent confirmation of this CR production rate is obtained from the observed correlation of O and Be abundance.

The other direct tests of the existence or non-existence of a hot, dense phase of cosmic evolution have similarly been demonstrated to be consistent with GOLE. The antimatter/baryon non-conservation problem is eliminated without BBH, as pointed out in section 5. Combined with the hypothesis of energy loss of EM radiation, non-BB evolution also correctly predicts the constancy of surface brightness, and this constancy has now been confirmed by the entirely independent analysis of Whitney et al (2020). In section 6 the SN1a luminosity- distance relationship predicted by the non-expansion hypothesis is shown to be closer to the SN1a data once the newly-discovered correlation of SN properties with galactic age is taken into account. In section 7 for the first time it is demonstrated that, when the galactic age dependence is taken into account, SN1a observed widths are constant with z, in accord with non-expansion predictions and in contradiction with BBH. In all of these additional direct tests, predictions based on BBH are contradicted by the data, and those based on no hot, dense phase of evolution (which we refer to as GOLE) are confirmed by the data.

Other data sets have been cited in support of the BBH, specifically observations of the CMB. It is widely argued that the energy density, isotropy and black body spectrum of the CMB can't be explained by anything other than the BBH.

However, in section 4.2 we show that the energy generated in the production of the observed amount of He is comparable to, and might even exceed, the observed energy in the CMB, so this energy density does not require the BBH. The isotropy and black-body spectrum of the CMB are evidence not specifically for a hot dense stage of cosmic evolution, but are instead evidence that the universe at some point in its history had a high optical depth in the microwave band. There is convincing evidence first published in 1990 (Lerner 1990, 1993) and elaborated in Lerner, 2021a, that the present universe has this high optical depth in this wavelength range, so no past high-density epoch is required. Specifically, these papers show that the luminosity in the radio waveband of galaxies with a given IR luminosity falls rapidly with increasing distance from earth. This fall occurs with 600 Mpc of earth, in a distance that is impossible to explain by any evolutionary change. This observational evidence can only be explained by an absorption or scattering of radio-band radiation in the IGM which can account for a high optical depth in the microwave band in the present-day universe, eliminating the need for a high-density phase in the past. Lerner, 1992, describes in detail a plasma mechanism for the absorption and re-emission of microwave-band radiation by magnetized filaments in the IGM. Thus, known processes occurring in the present-day universe can account for the main features of the CMB.

At the same time, the quantitative predictions of the BBH model of the CMB have been increasingly contradicted by observation. The CMB fluctuations are not Gaussian on the largest scales as BBH requires (Schwarz, 2016); the largest-scale modes are a poor fit to BBH predictions (Schwarz, 2016), and the CMB fluctuations are not best fit by the flat universe required by BBH inflation (Handley, 2019, Park&Ratra 2019, DiValentino et al, 2020). Finally, as has been widely noted, the BBH predictions of the Hubble relation, based on the CMB, are wrong(Riess, 2020), as are the best-fit predictions of matter density (DiValentino et al, 2020). Thus, not only is the BBH not required to explain the CMB, its specific quantitative predictions are at present in contradiction with observation.

In assessing whether the BBH or GOLE is valid it is important to note that observations over, especially, the last five years demonstrated a growing number of additional contradictions between other BBH predictions and observations, specifically involving the "age problem" and structure formation with dark, non-baryonic, matter (DM). The age problem is the existence of objects in the universe that are older, in some cases far older, than the time since the hypothesized Big Bang (Lerner, 2022; Wang, Li &Li, 2010). In addition, BBH structure formation requires the existence of DM. This DM hypothesis itself has encountered growing contradictions with observations including no lab evidence of DM particles (Adhikari, *et al.*, 2018; Aprile *et al.* (XENON Collaboration), 2018; Liu, Chen, & Ji, 2017); evidence against DM dynamic viscosity(Oehm &Kroupa, 2018); disk alignments of galaxy satellites (Santos-Santos, Domínguez-Tenreiro,& Pawlowski, 2019; Müller et al., 2018); and no DM in small galaxies (Mancera Pina *et al*, 2019).

Such age problems do not exist for the GOLE hypothesis, which eliminates the hypothesis of an initial dense, hot epoch for the universe. By including the well-known effect of magnetic fields and electric currents, and by discarding the BBH, including DM, the main features of the formation of cosmic structure have been accurately predicted (Alfven, 1978, 1981; Lerner, 1986; 2022) The application of this model to the early stage of galaxy formation leads to the GOLE hypothesis (Lerner, 1988, 1989).

At the present time, no predictions of the BBH are in quantitative agreement with subsequently published observational date, except the D abundance predictions. There are at least 16 independent observational contradictions to these predictions (Table 2). This extremely poor performance of BBH exists despite the fact that the BBH currently requires at least four hypotheses not based on laboratory-validated physics: the inflation field, non-baryonic matter (DM), dark energy and baryonic non-conservation. The GOLE hypothesis, in contrast, requires only one new hypothesis—that EM radiation loses energy as it travels long distances.

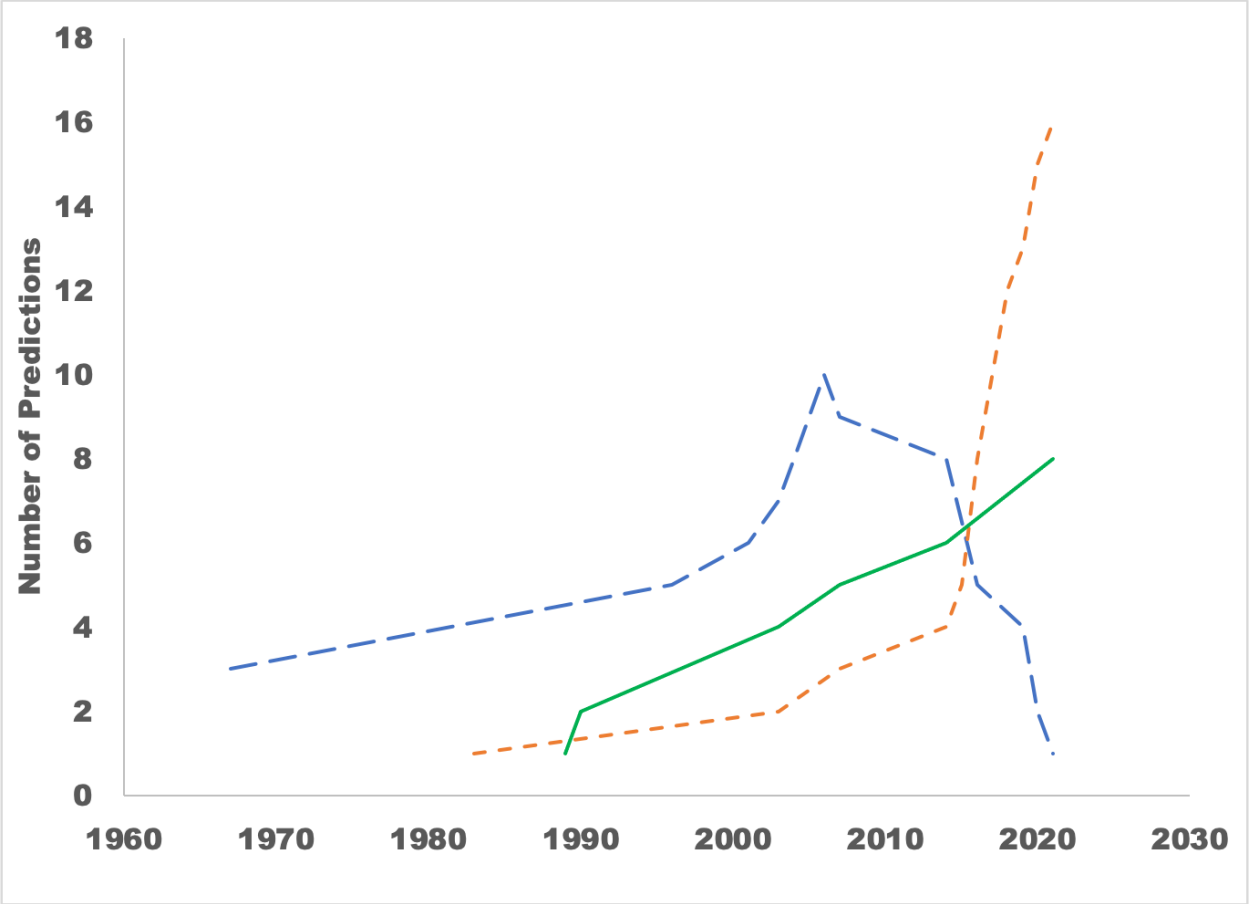

Figure 23. Number of independent predictions of BBH that were reported in peer-reviewed papers as verified by observations made after the predictions, against the year (long-dashed line). Number of BBH predictions that were contradicted by observations, as reported in peer-reviewed journals (short-dashed line). The data is the same as that in Table 2. Number of confirmations of GOLE predictions in peer-reviewed journals (solid line) based on the data in Table 3

This situation has developed mainly over the last seven years. Before about 2015, it could be argued on the basis of peer-reviewed publications that BBH had more verified predictions than observational contradictions, that contradictions were isolated "anomalies" in a generally well-supported theory. In Fig 16, we plot the number of independent predictions of BBH that were reported in peer-reviewed papers as verified by observations made after the predictions, against the year (long-dashed line). Similarly, we plot the number of BBH predictions that were contradicted by observations, as reported in peer-reviewed journals (short-dashed line). When new data contradicts predictions previously reported as confirmed, the total number of confirmed predictions decreases accordingly. The data is the same as that in Table 2. By 2006 there were 10 independent confirmations of BBH predictions reported in the literature and only two clear contradictions, to the Li and He data. We also plot the number of confirmations of GOLE predictions in peer-reviewed journals (solid line) based on the data in Table 3. As of 2006, there were four independent predictions of GOLE reported as confirmed by subsequent observations.

A number of researchers, including the present author (Lerner, 1993), had published critiques of the validity of many of these claimed confirmations, including questioning the methodology of introducing ad-hoc concepts such as dark energy. However, the number of reported confirmed BBH predictions remained well above the number of clear-cut contradictions in the first decade of the century.

In 2014, this situation began to change at an accelerating pace. Analyses of surface brightness data showed unequivocal contradiction with BBH predictions (Lerner, Falomo, Scarpa 2014) and the release of Planck data confirmed many contradictions with the CMB predictions of BBH (Schwarz, 2016). Deeper surveys revealed large scale structures incompatible with BBH age predictions (Shirokov et al, 2016). Multiple contradictions with DM predictions were reported, as noted above. Finally, in the 2019-2020, widely-publicized contradictions with BBH predictions of the Hubble constant, based on the CMB, led to widespread acknowledgment of a "crisis in cosmology" (DiValentino et al, 2020). In the present paper, the SNIa widths are added to the list of contradictions. During the same period, three independent predictions of the GOLE theory were confirmed, and there have continued to be no published contradictions of any GOLE predictions, as documented in the present papers.

At present, the focus of researchers' attention has remained overwhelmingly on the contradictions with BBH predictions arising from the CMB data. Both the long-standing contradictions with Li and He predictions and the more recent contradictions with surface brightness, large scale structure and DM have been largely ignored. This is to a certain extent a product of the specialization of the field, in which many researchers are simply unaware of developments outside their own area of research. The present paper and the author's recent paper on structure formation (Lerner , 2022) constitute a first attempt to overcome this problem and bring together the new results reported here with previously-published results to show the true situation of the BBH and GOLE alternatives.

Given that the accumulation of contradictions of BBH predictions in all of these data sets over the past eight years, the obvious question is why the BBH remains the accepted model, used by the vast majority of cosmology researchers. It should be clear from the summaries in this paper and the extensive literature that they rest on, that the answer does not lie in the scientific validity of the hypothesis, which has clearly been falsified by observation. It lies instead in the sociology of science.

As Merritt, (Merritt, 2017), among others, has pointed out, the field of cosmology has for a long time taken a "conventionalist" approach. Instead of seeking to validate or falsify scientific hypotheses, the conventionalist approach takes certain paradigms as given or "orthodox" and defends them against multiple falsifications by observation. It does this with methods such as ad-hoc hypotheses, treating contradictions as isolated "anomalies" or by simply ignoring them.

The standard answer to each of the severe contradictions enumerated in table 2 is "BBH is overwhelmingly confirmed by many other data sets, so this one is just an anomaly that has not yet been explained." Such a gross violation of the scientific method of course blocks progress in this field, as occurred for centuries with the Ptolemaic cosmology.

To overcome this widespread, but unscientific response, it has been essential in the present paper to comprehensively present in a single place a full comparison with all data sets of the BBH and the alternative—the abandonment of the BBH. This admittedly results in a lengthy paper, but is unavoidable in the present state of cosmological discussion.

It is also the reason why this paper must be published on Arxiv, rather than in a peer-reviewed publication. It is against the policy of leading peer-reviewed publications to publish such a paper. An earlier version of this present paper was rejected by MNRAS, for example, after a long review process, in which I satisfied all of the reviewer's major objections, (and all but one of the minor objections). The anonymous senior editor rejected the paper, writing that "*There are many journals which would be interested in publishing a well-argued synthesis of existing evidence against the standard hot big bang interpretation. But MNRAS, with its focus on publication of significant new astronomical results, is not one of them."* I confirmed with Dr. Flowers, the editor-in-chief, that this is indeed MNRAS's policy.

The reaction of researchers to the growing contradictions with observation that has become widely acknowledged as the "crisis in cosmology" also reflects a conventionalist approach. Instead of viewing the multiple contradictions of predictions by observation as falsifications of the basic BBH, paper after paper proposes additional ad-hoc assumptions such as early dark energy, new early dark energy, phenomenologically emergent dark energy, interacting dark energy, fuzzy dark matter, decaying dark matter dark forces and so on. This drives cosmology into a dead-end.

It is important to note that the adoption of any of the elaborations on dark energy, even if they were to conform to all existing data, would entirely destroy the predictive power of the BBH. While previous additions to the BBH have added one free parameter at a time, the adoption of new concepts of dark energy would be chosen from among an infinite set of possible functions. Since any predictive theory has to have fewer free parameters than independent observations, the adoption of a theory with an infinite set of free parameters would eliminate BBH as a predictive and thus scientific theory.

But the overwhelming adherence to this conventionalist approach raises the deeper question—why has cosmology, in particular among scientific fields, become paralyzed for decades by this conventionalist straightjacket? In other fields of science, dearly-held and entrenched paradigms have been overthrown, but not in cosmology, despite decades of deepening observational contradictions, and the existence of an alternative hypothesis—namely, the simple rejection of the Big Bang hypothesis.

It is beyond the scope of this article to discuss in full the reasons for this rigidity, which has been explained in detail elsewhere (Alfven, 1978, Lerner, 1992, López Corredoira & Perelman, 2008). However, two key points should be briefly outlined. First, in almost all fields of science, the ultimate test of validity is in the application to technology. The validity of Maxwell's equations is demonstrated each time a light switch is thrown, those of quantum mechanics every time you look at a computer screen. The effectiveness of new paradigms in technology ultimately drives acceptance.

Cosmology in the past half century and more has appeared to be effectively isolated from applications to technology. While discoveries in astrophysics in the past had obvious implications for technology, such as the discovery in the 1930's of nuclear fusion as the source of energy of the stars, no such links are widely recognized today. The real links that do exist between plasmas in the cosmos and those on earth are unknown to all but a few researchers in cosmology. So, the possibility of paradigm change as demonstrated by technological advances has been absent.

Second, and even more important, is the concentration of the funding for cosmological research in a very small number of sources. In other fields of science, a variety of funding sources, including many different governmental sources, allow for a diversity of models. But in cosmology, largely because of its perceived lack of application, such numerous different funding sources don't exist.

Funds for astronomical research and time on astronomical satellites are allocated almost exclusively by very few governmental bodies, such as the National Science Foundation (NSF) and National Aeronautics and Space Administration (NASA) in the United States. The review committees that allocate these funds are tightly controlled by adherents of the Big Bang theory, who refuse to fund anything that calls their life's work into question. It is no secret that, today, anyone who questions the Big Bang, who develops alternatives to the Big Bang, or, for the most part, who even investigates evidence that contradicts the Big Bang, will not receive funding.

This concentration of funding sources creates a strong "Emperor's-New-Clothes" effect where those who don't see the beauty of the BBH are deemed incompetent and thus unworthy of funding. It should be remembered that it was only the Emperor's unquestioned power over people's livelihoods that led to the dominant theory that the clothes were beautiful.

In Anderson's immortal fable, it is ridicule that finally undoes the Emperor. Given the widespread attention to the Crisis in Cosmology, perhaps researchers will soon see the inflationary ΛCDM Big Bang (with its contradictions to 16 different sets of data) as equally, or more, ridiculous than the fictional Emperor. Perhaps at that point the funding of cosmology can be reformed to be more diverse and less dominated by conflicts of interest. Certainly, having funding requests reviewed by astrophysicists from *outside* the field of cosmology would be a first step the right direction.

The only route out of the crisis is to recognize that BBH has in recent years been falsified. This route would then involve elaborating and testing against observations a cosmological model without a Big Bang. A number of tasks on this route are clear right now. Uncertainties in the theory of light elements production can be reduced through observations of stars and planetary nebulae, as well of as young galaxies (ULIRGS). Modeling of stellar evolution of initially pure H stars is also needed. Observational tests can be devised to better constrain the production of cosmic rays by stars of different masses. For the CMB, extensive modeling, with significant resources, is needed to compare with observations the power spectrum and other features of a predicted CMB produced by thermalized stellar radiation and scattered by the IGM. As pointed out in section 6, space-based experiments are possible to directly test the hypothesis that EM radiation loses energy with distance. On this route, the crisis in cosmology will be resolved on

the basis of known physical laws and observations, paving the way to a model that makes increasingly useful predictions of subsequent observations.

Table 2. Predictions of BBH

data set/Prediction	year confirmation	ref	year earliest contradiction	ref	observed conflict at present	ref for conflict at present
Li abundance	1967	Wagoner, Fowler and Hoyle ,1967	2003	Cyburt, Fields and Olive, 2003	observed 1/20 predicted	Fields et al (2020)
He abundance	1967	Wagoner, Fowler and Hoyle ,1967	2007	Casagrande, et al, 2007	observed 1/2 predicted	Portinari, Casagrande and Flynn 2010, Maciel, Costa and Cavichia 2017
D abundance	1967	Wagoner, Fowler and Hoyle,1967				
surface brightness dimming	1996	Pahre, Djorgovski & de Carvalho,1996	2014	Lerner, Falomo, Scarpa 2014	>5σ	Lerner, 2018
large scale Gaussainity CMB	1996	Bennett et al, 1996	2016	Schwarz, 2016	>4.4σ	Schwarz, 2016
SNI a widths	2001	Goldhaber,2001	2021	this paper	>7.5σ	this paper
CMB predictions of H0	2003	Hinshaw et al, 2003	2020	Riess, 2020	>4.5σ	Riess, 2020
CMB prediction of matter density	2003	Hinshaw et al, 2003	2020	DiValentino et al, 2020	>3.5s	DiValentino et al, 2020
Large Scale Structure size	2004	Tegmark, et al, 2004	2016	Shirokov et al, 2016	>6 times larger than predicted	Shirokov et al, 2016
fit of CMB large-scale modes	2006	Sanchez, et al, 2006	2016	Schwarz, 2016	>3.3σ	Schwarz, 2016
CMB fit to flat universe	2006	Sanchez, et al, 2006	2019	Handley, 2019, Park&Ratra 2019	>3.4s	DiValentino et al, 2020
proton decay/matter density			1983	Sreekantan,1984	no decay detected	Tanaka *et al*, 2020
galaxy dynamical masses less than stellar masses			2015	Peralta de Arriba *et al* ,2015	stellar masses>8x dyn mass	Peralta de Arriba *et al* ,2015
galaxy merger rate			2018	Lerner, 2018	1/10 predicted rate	Lerner, 2018
DM dynamical viscosity			2018	Oehm &Kroupa, 2018	numerical value not given	Oehm &Kroupa, 2018
DM galaxy sattelites distribution			2018	Muller et al., 2018	>3σ	Muller et al., 2018
DM in small galaxies			2018	Mancera Pina *et al*, 2019	numerical value not given	Mancera Pina *et al*, 2019

Table 2. Key quantitative predictions of the BBH. The second column shows the year in which peer-reviewed journals first published evidence that the predictions were confirmed by data published after the predictions were made. The third column show the year in which such journals first published evidence that the same predictions were contradicted by more recent data.

Table 3. Predictions of GOLE

data set/Prediction	year confirmation
Large Scale Structure-nr relation	1989
Radio-IR absorption	1990
Li abundance	2003
D abundance	2003
He abundance	2007
surface brightness constancy	2014
SNIa luminosity-distance	2021
ULIRG luminosity	2021

Table 3. Key quantitative predictions of the GOLE. The second column shows the year in which peer-reviewed journals first published evidence in papers by the present author that the predictions were confirmed by data published after the predictions were made.

10. Conclusions

A re-analysis of data and predictions of the galactic origin of light elements (GOLE) hypothesis almost 40 years after it was first proposed confirms that it has accurately predicted light element abundances. Its predictions, assuming the nonexistence of a hot, dense period of cosmic

evolution, have as well been confirmed by many other data sets. Only a single new assumption of EM energy loss with distance is required. No incompatibilities with data have been found.

In contrast, almost 60 years after the Big Bang hypothesis was proposed for the origin of light elements, observations have increasingly diverged from its predictions for He and Li abundances, leaving only D as a correct prediction. The Big Bang hypothesis' other predictions have been abundantly contradicted by at least 16 data sets, with divergence between prediction and observation increasing greatly over the past several years. Other than D abundance, the Big Bang predictions are not in accord with any data sets. Observations, taken as a whole, clearly exclude the hypothesis of a hot, dense (Big Bang) phase of universal evolution. The only solution to the crisis in cosmology is to recognize that the Big Bang never happened.

Acknowledgments

The author wishes to thank Dr. David Crawford, Dr. Walter Maciel and Dr. Lingyu Wang for sharing their data with me. This work was funded by LPPFusion, Inc.

Data Availability

The data newly analyzed in this paper was provided by permission of Dr. David Crawford, Dr. Walter Maciel and Dr. Lingyu Wang is available upon request to them.

References

Aartsen M. G., et al, 2020, arXiv:2001.09520v1
Abdalla, E., et al ,2022, Journal of High Energy Astrophysics, 34, 49
Ackermann M. et al., 2015, ApJ, 799, 86
Ackermann M. et al, 2017, ApJ, 835,219
Adhikari, G., et al., 2018, Nature 564, 83
Alfvén, H., 1939, Phys. Rev. 55, 425
Alfvén, H., 1978, Astrophys Space Sci 54, 279
Alfvén, H., 1981, Cosmic Plasma, (Holland, Reidel)
Alfven, H. and Klein, O.,1962, Arkiv f. Fysik, 23, 187
Aprile, E. et al. (XENON Collaboration), 2018, Phys. Rev. Lett. 121, 111302
Arnett, W.D., 1978, ApJ, 219, 1008
Assef, R. J., 2011ApJ, 728, 56
Audouze, J. & Silk, J, 1983, Proc. ESO Workshop on Primordial Helium, 71
Audouze, J., & Tinsley, B.M., 1976, Ann. Rev. of Ast. and Astrophys. 14, 43
Audouze, J., Lindley, D., Silk, J. 1985, ApJ, 293, L53
Baiesi, M., 2020,Phys. Rev. Research 2, 013210
Balescu, R., 1988, Transport Processes in Plasmas, (North Holland Publishing) p.211
Bennett, C.L. *et al*, 1996, ApJ, 464,L1
Bennet, C. L. et al Astrophys., 2003, J.Suppl.148:1
Bonofacio, P., et al, 2015, A&A 579, A28
Brown, T. and Wilson, C.D., 2019, ApJ 879 17

Burbidge, E.M., Burbidge, G. R., Fowler, W. A. and Hoyle F. ,1957, Rev. Mod. Phys. 29, 547
Caffau,E. et al ,2011,Nature 477, 67–69
Casagrande, L., Flynn, C., Portinari, L, Girardi, L., Jimenez, R., 2007, MNRAS 382, 1516
Chiu, H.Y., Phys Rev. Lett, 1966, 17, 610
Ciprijanovic, A., 2016, Astroparticle Physics 85, 24
Cole, S., Lacey, C. G., Baugh, C. M., & Frenk, C. S. 2000, MNRAS, 319,168
Copi, C. J., Huterer, D. ,. Schwarz D. J., & Starkman, G. D., , 2015,MNRAS 449, 3458
Crawford D. F., 2017, Open Astronomy, 26, 111
Cummings A. C., et al, 2016, ApJ 831,18.
Cyburt,R.H., Fields, B.D. and Olive,K.A., 2003, Phys.Lett.B567:227-234
deRutier, H.R,1990, A&A 227, 351
Deveraux, N.A., & Eales, S. A., 1989,ApJ, 340, 708
Di Valentino, E., Melchiorri, A. & Silk J., 2020, Nature Astronomy 4, 196
Doherty, C.L., Gil-Pons,P., Lau,H.H.B., Lattanzio, J.C., & Lionel Siess, L. ,2014, MNRAS 437, 195
Dowell J. & Taylor, G. B. 2018,ApJL, 858, L9
Draine B. T., Lazarian A., 1998, ApJ, 494, L19
Eker, Z. et al, 2018, MNRAS, 479, 5491
Eser, E. K., Goto, T. and Doi, Y., 2014, ApJ 797, 54
Fan L., Lapi A., De Zotti G., Danese L., 2008, ApJ, 689, L101
Ferland, G. J. 1986, ApJ. Letters 310, L67
Fiege, J.D., & Pudritz, R.E., 2000, MNRAS, 311, 85
Fields, B.D. et al JCAP03(2020)010
Fields, B.D., & Prodanovic, T., 2005, ApJ 623, 877
Fontes, P. Thesis 1570, 1975, Univesite de Paris, Centre d'Orsay
Frebel A., et al, 2008, ApJ, 684,588
Frebel, A. et al 2019, arXiv:1810.01228v1
Fushiki,I. & Lamb, D. Q., 1987, ApJ, 317, 368
Gallazzi, A., Brinchmann, J., Charlot, S., White, S. D. M. 2008, MNRAS, 383, 1439
Gamow, G., 1946, Phys. Rev. 70, 572
Georgi, H., Quinn H. R. and Weinberg, S. ,1974, Phys. Rev. Lett.33, 451
Gilmore, G., Edvardsson, B., Nissen, P.E., 1991, ApJ 378, 17
Goldhaber, G., et al, ApJ, 2001, 558,359
González Hernández J. I. et al, 2008 A&A 480, 233
Handley W., 2019, arXiv e-prints, p. arXiv:1908.09139
Hansen T. et al ,2015,ApJ, 807,173
Haslam, C. G. T. et al, 1981, A&A 100, 209
Hensley B.S., Draine, B. T. & MeisnerA.M, 2016 ApJ 827 45
Hinshaw, G. *et al*, 2003, ApJ Supp,148,135
Howell T. F. & Shakeshaft, , , J. R. 1967,Nature 216, 753
Howk, C. Lehner, N. , Fields , B.D., & Mathews G.J., 2012, Nature 489, 121
Hoyle, F. and Taylor, R.J., 1964, Nature 203, 1108
Hoyle, F., 1946, MNRAS 106, 343
Huba,J.D., 2013, NRL Plasma Formulary, (Naval Research Laboratory) p.28
https://library.psfc.mit.edu/catalog/online_pubs/NRL_FORMULARY_13.pdf
Izotov, Y.I., Thuan, T.X., and Lipovetsky, V.A., 1997, Ap. J. Sup., 108:1,

Kang, Y., Lee, Y.-W., Kim, Y.-L., et al. 2020, ApJ, 889, 8
Karachentsev, I.D., 2012, Astrophys. Bull., 67, 123
King, C.H.,1975, Phys. Rev. Lett. 35, 988
Kipling, R., 1912, Just So Stories, Konecky and Konecky
Koay, J. Y., Jauncey, D. L., Hovatta, T., Kiehlmann, S., Bignall, H. E., Max-Moerbeck, W.T., Pearson, J., Readhead, A. C. S., Reeves, R. ,Reynolds, C. ,Vedantham, H., 2019, MNRAS 489, 5365
Kotelnikov, I.A., 2012, Plasma Physics Reports, 38, 608
Krisciunas, K., 1993 , J. Royal Astr. Soc. Can., 87, 223
Kroupa, P. Pawlowski, & M. Milgrom, M., 2012 Int. J. Mod. Phys. D 21,1230003
Lee,Y-W., Chung,C. , Kang,Y.& Jee,M.J., 2020, arXiv:2008.12309
Lehnert, B., 1978, Astrophys and Space Sci., 53, 459
Leitch E. M., Readhead A. C. S., Pearson T. J., Myers,S. T., 1997,ApJ, 486, L23
Lemaitre, G., 1931, Nature 127, 706
Lerner, E.J., 1986, IEEE Trans. Plasma Sci. 14, 690
Lerner, E. J., 1988, Lasers and Particle Beams, 6, 457
Lerner , E.J., 1989, IEEE Trans. Plasma Sci. 17,259
Lerner, E. J., 1990, Ap. J.,361, 63
Lerner, E.J., 1992, IEEE Trans Plasma Sci., 20, 935
Lerner, E.J. 1993a, Astrophys& Space Sci., 207, 17
Lerner, E.J., 1993b,"The Case Against the Big Bang" in Progress in New Cosmologies, H.C. Arp et al, editors, Plenum Press
Lerner E. J., 2006, AIP Conference Proceedings, 822, 60
Lerner E. J., 2009, ASP Conference Series, 413, 12
Lerner E. J, 2018, MNRAS, 477, 3185
Lerner, E.J. 2022, https://www.lppfusion.com/storage/Structure-Lerner.pdf
Lerner E. J., Falomo R., Scarpa R. 2014, Int.J.Mod.Phys. D23 6, 1450058
Li,H. Aoki,W., Zhao,G. Honda,S. Christleib, N. and Suda, T., 2015, Publ. Astron. Soc. Japan 67
Liu, J., Chen, X. & Ji, X., 2017, Nature Phys 13, 212
Lopez, J. L., Nanopoulos, D. V. and Pois, H. 1992, AIP Conference Proceedings 272, 1395
Maciel, W. J., Costa, R. D. D., Cavichia O. ,2017, Journal of Physics: Conf. Series 940, 012045
Mancera Pina, P.E., *et al,* 2019, ApJL 883**,** L33
Marassi, S. ,2019, MNRAS, 484, 2587
Mathews, G. J., Boyd, R.N., and Fuller, G.M.,1993 ApJ 405, 65
Mathews, G. J., Kusakabe, M. , Kajino. T., 2017, Int J.Mod.Phys. E26, 1741001
Mathews, G.J., et al (2020) JPS Conf.Proc. 31 011033
Matsumoto et al, 2022, arXiv:2203.09617v1
Matsuno, T. et al ,2017a, AJ 154 52
Matusno, T., Aokio,W. Suda,T.and Li, H. , 2017b, Publ.Astron.Soc.Japan 69 (2), 24 (1)
Mazziotta, M.N., 2016, Astroparticle Physics 81, 21
Melendez, J., et al , 2016,A&A 585, L5
Melnick, J. , Heydari-Malayeri, M. Leisy, ,P., 1992, A&A 253, 16
Meneguzzi, M., Audouze, J. & Reeves, H., 1971, A&A, 15,337
Mercer, D.J., et al, 2001, Phys. Rev. C 63, 065805
Merritt, D., 2017, Studies in History & Philosophy of Modern Physics, 57, 41
Millikan, R. A. and Cameron, G. H., 1929, Phys. Rev. 32, 533

Mo H. J., Mao S., & White S. D. M. ,1998, MNRAS, 295, 319
Müller *et al*., 2018, Science 359, 534
Naab T., Johansson P., & Ostriker J.P., 2009, ApJ, 699, L178
Nicholson, et al, 2016, Nature Communications, 6, 6896
Nissen P. E., Chen,Y. Q., Carigi, L., Schuster, W.J. & Zhao,G.,2014, A&A 568, A25 W. J.
Nordlander, L. et al, 2019, MNRAS, 488 L109
Odegard, N.Weiland, J. L., Fixsen, D. J., Chuss, D. T., Dwek, E., Kogut, A., Switzer, E. R., 2019, ApJ 877, 40
Oehm, W and Kroupa, P. In *Conference Cosmology on Small Scales 2018 p.30,* Institute of Mathematics CAS, Prague
Oosterloo, T.A.,Vedantham, H. K., Kutkin, A. M., Adams, E. A. K., Adebahr, B., Coolen, A. H. W. M., Damstra, S., de Blok, W. J. G., Dénes, H., Hess, K. M., *et al*, . 2020A&A 641, L4
Pahre, M. A. Djorgovski S. G. & de Carvalho R. R., ,1996, Astrophys. J. 456 L79
Park C.-G., Ratra B., 2019, ApJ, 882, 158
Peebles, P.J. E. and Yu, J.T., 1970 ApJ 162, 815
Peralta de Arriba L. et al 2015, MNRAS, 453, 704
Pereira-Santaella, M., Rigopoulou1, D., Farrah D., Lebouteiller V., Li J., 2017, MNRAS, 470, 1218
Peter, W. & Peratt, A.L., 1990 IEEE Trans. Plasma Sci., 18,49
Piau L. et al ,2006, ApJ, 653:300
Planck Collaboration, 2020, A&A 641, A6
Portinari, L. Casagrande L. and Flynn C. ,2010, MNRAS 406, 1570
Primack ,R., 1995, arxiv/9503020
Pringle, J. E., Ronald P., Allen, J.& Lubow S. H., 2001, MNRAS, 327, 663
Ramaty,R. & Lingenfelter, R. E. ,1969, ApJ 155, 587
Raskin, C. Scannapieco, E., Rhoads, J. & Della Valle, M., 2009, ApJ, 707,74
Riess, A. ,2020, Nature Reviews Physics, 2, 10
Ryan, S.g., Norris, J.E., Bessle, M.S. and Deliyannis, C.P., 1992, ApJ 388, 184
Sajina A., Yan, L., Fadda, D., Dasyra, K. & Huynh M., 2012,ApJ, 757,13
Sanchez, A.G., et al, 2006, MNRAS 366, 189
Santos-Santos, I.M., Domínguez-Tenreiro, R., Pawlowski, M.S. ,2019, https://arxiv.org/abs/1908.02298v1
Sbordone, L. et al. 2010 A&A 522
Schwarz D. J., Copi, C. J., Huterer, D., & Starkman, G. D, 2016, Class. Quantum Grav. 33, 184001
Schwarz D J, Starkman G D, Huterer D & Copi C.J., 2004, Phys. Rev. Lett. 93, 221301
Shibuya T., Ouchi M. , Kubo M., Harikane Y. 2015, Ap.J. Sup. Ser. 219, 15
Shirokov, S. I., Lovyagin, N. Yu., Baryshev, Yu. V.,Gorokhov V. L, 2016, Astronomy Reports, 60, 563
Siess, L., 2010, A&A 512, A10
Soppera, N., Dupont E., Bossant M., Fleming M. ,2018, JANIS Book of proton-induced cross-sections, OECD NEA Data Bank
Spite, F. and Spite, M., 1982, A & A, 115, 357
Spite, M. et al 2019, A&A 624, A44
Sreekantan, B. V., 1984, J. Astrophys. Astr. 5, 251

Steigman, G. , 1995, in Particles, Strings And Cosmology - Proceedings Of The John Hopkins Workshop ,edited by Domokos Gabor, Kovesi-domokos Susan, Bagger Jonathon A , World Scientific
Steigman, G., & Walker, T.P., 1992 Ap J 385, L13
Sun, W. 2015, Thesis, Precision Measurement of the Boron to Carbon Ratio in Cosmic Rays with AMS-02, MIT
Takahashi, K. Hideyuki Umeda, H. & Yoshida,T. , 2014, ApJ 794 40
Tan, K. F. Shi, J. R. & Zhao G., 2009, MNRAS, 392, 205
Tanaka , M. et al, 2020, Phys. Rev. D 101, 052011
Tegmark, M. et al, 2004, ApJ 606,702
Telesa, S. Amanda R.Lopesb, A.R. & Ribeiroa, M.B. , 2021, Phys. Lett.B 813,136034,
Whittam, I. H., Riley, J. M., Green, D. A., Jarvis, M. J.,& Vaccari, M., 2015,MNRAS, 453,4244
Tognelli, E., et al, 2020, A&A 638, A81
Tolman R. C., 1930, Proc, Natl. Acad. Sci., 16, 511
Tolman R. C., 1934, Relativity Thermodynamic and Cosmology (Oxford: Oxford University Press)
Valcarce, A. A. R., Catelan, M. & De Medeiros, J. R., 2013,A&A 553, A62
van der Wel A., et al, 2014, ApJ, 788, 28
Ventura, P., et al, 2014, MNRAS 437, 3274
Vida-Madaj,A. & Gry, C.,1984, A & A, 138, 285
Wagoner, R.V., Fowler, W.A. and Hoyle, F. ,1967, ApJ, 148, 3
Walker, T.P., Mathews, G.J., Viola, V.E, 1985, ApJ 299, 745
Walker, T.P., Steigman, G., Schramm, D.N., Olive, K.A., and Kang, H., 1991, ApJ, 376,51
Wang, L., Gao, F., Duncan, K. J.,Williams, W. L., Rowan-Robinson, M., Sabater, J., Shimwell, T. W., Bonato, M., Calistro-Rivera, G., Chyży, K. T., Farrah, D, *et al*, 2019, A&A 631, A109
Wang, S., Li, X-D,, Li, M., 2010, Phys.Rev.D 82, 103006
Whitney, A., Conselice, C. J , Duncan K, & Spitler, L. R.,2020, arXiv:2009.07295
Yang, J., Turner, M.S., Steigman, G. , Schramm, D.N., and Olive, K.A. 1984 ApJ, 281, 493
Yeung, S. and Chu, M.-C., 2022, Phys Rev. D 105, 083508
Yoshimori, M., 1990, ApJ Supp, 73: 227
Yuan, Q. 2019, Science China Physics, Mechanics & Astronomy 62, 49511